

# Updated Results on Arterial Pressure Waveform Processing

Richard J. Kozick\*

February 25, 2001

New results in this update include the following:

- Automatic detection of the dichrotic notch is performed on the mean “decay” pulse. The algorithm for notch detection is based on a goodness-of-fit measure for a monoexponential fit to the distal part of the curve. That is, moving from systole to diastole, we seek the leftmost point that provides a “good” fit to a monoexponential model. The goodness-of-fit measure is root-mean-squared (RMS) error.
- The mean full-cycle pulse is obtained, and this pulse is passed through the inverse transfer function (TF). The published forward TF is interpolated with a cubic spline to obtain the inverse TF at a denser set of frequencies. Then the FFT is used to obtain the result of passing the mean full-cycle pulse through the inverse TF. Some observations:
  - The zero-frequency component is amplified the most by the inverse TF. Does this make sense from the physiology?
  - The published forward TF has frequency components only to the ninth harmonic. I assumed that the inverse TF has *zero gain* at frequencies beyond the ninth harmonic. This seems reasonable, since the full-cycle pulse has most of its energy in the first few harmonics. Are there other alternatives for defining the inverse TF beyond the ninth harmonic?
- Results are presented based on five different data sets: subject IDs 3011623 and 3014681 (from Jo), and subject IDs 7010966, 7010150, 7016670 from Laurie.
- A Matlab program is available that can produce the plots shown in this report for other data sets.

The monoexponential model that is used to fit the mean decay curve from the dichrotic notch to diastole is

$$x(t_i) = Ae^{-\alpha t_i} + B, \quad i = 1, \dots, N. \quad (1)$$

The parameters  $A$ ,  $\alpha$ , and  $B$  are chosen to minimize the squared-error between the model (1) and the mean decay curve, and the time constant is  $\tau = 1/\alpha$ . The time samples  $t_1, \dots, t_N$  are spaced by  $T_s = 1/F_s = 5$  msec, where  $F_s = 200$  samples/sec.

---

\*kozick@bucknell.edu Phone: (570) 577-1129 FAX: (570) 577-1822

Next we discuss Figures 1–8 for data set 3014681. Four other data sets are included in the subsequent plots.

We begin with the following report summarizing the analysis of data set 3014681.

\*\*\*\*Report for Subject ID 3014681:

For 17 similar pulses, indices of (min, max, min) for full-cycle:

289	319	499
499	525	700
700	731	908
908	939	1108
1108	1140	1306
1306	1336	1506
1506	1533	1713
1713	1741	1920
2982	3011	3186
3186	3216	3396
3820	3847	4017
4017	4050	4224
4833	4861	5034
5034	5059	5232
5232	5261	5434
5434	5461	5636
5636	5664	5838

Mean decay curve: length = 167 (samples) = 0.8350 (sec), notch at sample 64

Exponential fit:  $(100.6141) \cdot \exp(-(4.3799)t) + (69.5212)$

Time constant = 0.2283 (sec.)

RMS error = 0.2324 (mm Hg) with 103 points in fit

Sum-of-squares of data points in fit = 650636.9104 (mm Hg)<sup>2</sup>

Mean full-cycle curve: length = 198 (samples) = 0.9900 (sec)

Estimated pulse rate from similar pulses = 60.9529 BPM

Pulse rate from header: Cuff = 58, Analysis = 58

Figure 1(a) shows the full waveform along with derivatives, and Figure 1(b) shows the detected maxima and minima. The algorithm for finding maxima and minima was described in the status report of January 14, 2001. Pulses are called “similar” if their cardiac cycle lengths (CCL) are within 5% of the mean value over the entire waveform, and if the preceding pulse also has a similar CCL. Figure 2(a) shows the 17 similar curves, along with the mean “decay” curve. The dichrotic notch is detected from the mean curve using the procedure described in the next paragraph, with the detected notch shown as the vertical line in Figure 2(a). Then Figure 2(b) shows the monoexponential fit of equation (1) to the mean curve in Figure 2(a) from the notch to diastole. The time constant and RMS error for the fit are given in the summary report listed above.

Figure 3 shows the mean decay curve from Figure 1(a) along with its derivatives, with and without smoothing. Note that the derivatives are noisy, so they are difficult to use

to detect the dichrotic notch. Since our goal is to fit an exponential model to the distal portion of the curve, a possible way to define the notch is the left-most point for which the exponential model is no longer valid. We consider candidate positions for the notch ranging from the first 1/4 of the curve (to the right of systole) to the last 1/3 of the curve (to the left of diastole). We compute an exponential model fit for each curve, and compute goodness-of-fit measures. Three such measures are plotted in Figure 4(a) versus the candidate notch offset: RMS error, normalized RMS error (normalized by the sum of squares of data points), and maximum absolute error. Note that sample 64 is a breakpoint for all three measures: moving further to the left produces a much worse fit to exponential model. Note from the vertical line in Figure 2(a) that sample 64 is a reasonable estimate of the dichrotic notch. The RMS error will be used as the goodness-of-fit measure to find the notch in subsequent analysis. Figure 4(b) shows that the exponential model parameters  $\tau = 1/\alpha, A, B$  in (1) vary significantly for different choices of the notch location, and that placing the notch at 64 is the “stable” point for which the distal curve follows an exponential model.

The algorithm used to find the dichrotic notch from the RMS error plot in Figure 4(a) is as follows: Moving from left to right, look for the first point where the RMS error is *less* than the RMS error on the 4 rightmost points, and the RMS error is less than the mean RMS error over the interval.

In Figure 5, we show the similar full-cycle pulses and the mean full-cycle pulse, from minimum to minimum. The mean full-cycle pulse will be passed through the inverse transfer function (TF), which is developed as follows. Figure 6(a) shows an estimate of the published forward TF, with values read from the published graphs. Figure 6(b) shows a cubic-spline interpolation of the estimated values, with amplitude gain set to zero for harmonics greater than 9. Figure 6(c) shows a cubic-spline interpolation of the estimated *inverse* TF, with amplitude gain set to zero for harmonics greater than 9. Figure 6(d) shows the FFT magnitude of the full-cycle mean pulse. Note that the harmonics beyond 10 Hz are 17 dB or more below the fundamental frequency.

Figure 7(a) contains the full-cycle pulse, after processing with the inverse TF. Figure 7(b) shows the original full-cycle pulse and the pulse after inverse transform on the same plot, with the peak amplitude normalized to 1. Figure 8 shows the impulse response (inverse Fourier transform) of the forward and inverse Fourier transforms.

The following data sets have been processed, with summary reports as listed and corresponding plots in the indicated figures:

- Data set 3011623: Figures 9–15.

\*\*\*\*Report for Subject ID 3011623:

For 13 similar pulses, indices of (min, max, min) for full-cycle:

311	351	512
512	555	706
1087	1128	1284
1284	1326	1482
1900	1948	2110
3172	3214	3369
3369	3410	3573

3573	3616	3775
4161	4206	4361
4361	4400	4556
4944	4980	5133
5523	5567	5730
5730	5775	5930

Mean decay curve: length = 152 (samples) = 0.7600 (sec), notch at sample 75  
 Exponential fit:  $(68.1447) \cdot \exp(-(3.6126)t) + (60.6966)$

Time constant = 0.2768 (sec.)

RMS error = 0.0949 (mm Hg) with 77 points in fit

Sum-of-squares of data points in fit = 379517.2027 (mm Hg)<sup>2</sup>

Mean full-cycle curve: length = 190 (samples) = 0.9500 (sec)

Estimated pulse rate from similar pulses = 59.8615 BPM

Pulse rate from header: Cuff = 60, Analysis = 59

- Data set 7010150: Figures 16–22.

\*\*\*\*Report for Subject ID 7010150:

For 7 similar pulses, indices of (min, max, min) for full-cycle:

311	339	531
1201	1223	1412
1412	1436	1629
1629	1657	1839
3583	3608	3794
3794	3817	4009
4009	4036	4228

Mean decay curve: length = 183 (samples) = 0.9150 (sec), notch at sample 104  
 Exponential fit:  $(45.4554) \cdot \exp(-(2.3947)t) + (77.6223)$

Time constant = 0.4176 (sec.)

RMS error = 0.1168 (mm Hg) with 79 points in fit

Sum-of-squares of data points in fit = 585145.3476 (mm Hg)<sup>2</sup>

Mean full-cycle curve: length = 211 (samples) = 1.0550 (sec)

Estimated pulse rate from similar pulses = 64.4143 BPM

Pulse rate from header: Cuff = 55, Analysis = 54

- Data set 7010966: Figures 23–29.

\*\*\*\*Report for Subject ID 7010966:

For 5 similar pulses, indices of (min, max, min) for full-cycle:

829	868	1030
2090	2126	2282

2282	2319	2475
2475	2511	2665
5274	5307	5464

Mean decay curve: length = 155 (samples) = 0.7750 (sec), notch at sample 59  
 Exponential fit:  $(70.5848) \cdot \exp(-(2.5332)t) + (47.3736)$   
 Time constant = 0.3948 (sec.)  
 RMS error = 0.3310 (mm Hg) with 96 points in fit  
 Sum-of-squares of data points in fit = 430044.9276 (mm Hg)<sup>2</sup>  
 Mean full-cycle curve: length = 191 (samples) = 0.9550 (sec)  
 Estimated pulse rate from similar pulses = 57.9600 BPM  
 Pulse rate from header: Cuff = 59, Analysis = 55

- Data set 7016670: Figures 30–36.

\*\*\*\*Report for Subject ID 7016670:

For 11 similar pulses, indices of (min, max, min) for full-cycle:

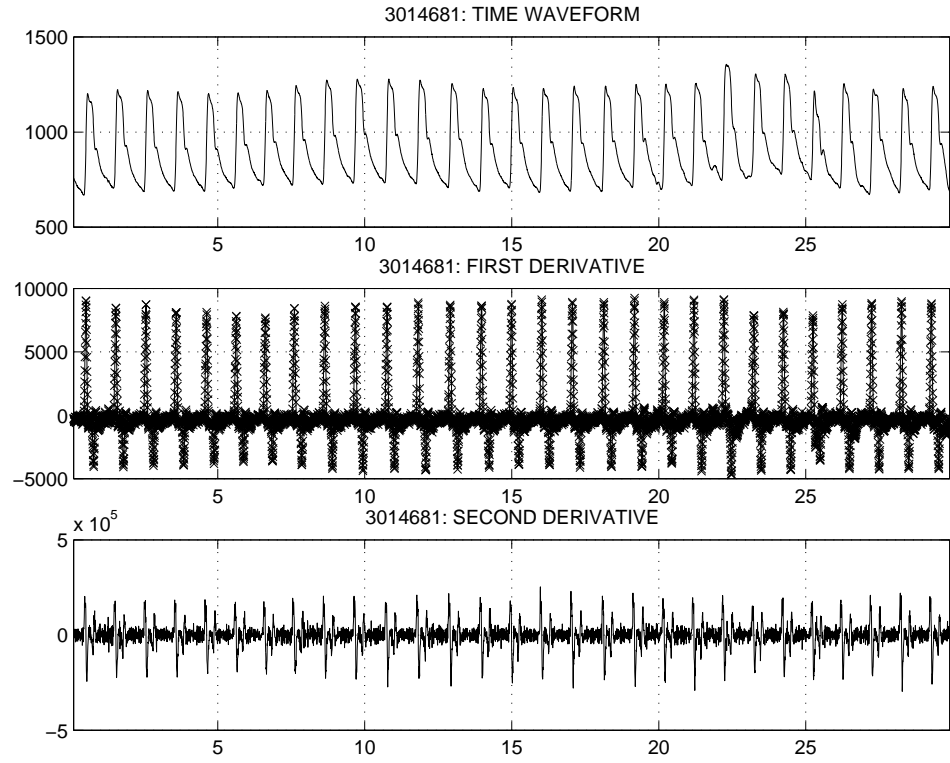
1351	1373	1556
1556	1579	1752
1752	1775	1947
2351	2378	2550
3358	3386	3562
3562	3591	3763
3763	3790	3967
3967	3996	4174
4174	4408	4585
4585	4610	4792
4792	5033	5212

Mean decay curve: length = 173 (samples) = 0.8650 (sec), notch at sample 77  
 Exponential fit:  $(136.2479) \cdot \exp(-(3.1476)t) + (63.6983)$   
 Time constant = 0.3177 (sec.)  
 RMS error = 0.3307 (mm Hg) with 96 points in fit  
 Sum-of-squares of data points in fit = 692277.3892 (mm Hg)<sup>2</sup>  
 Mean full-cycle curve: length = 196 (samples) = 0.9800 (sec)  
 Estimated pulse rate from similar pulses = 72.2455 BPM  
 Pulse rate from header: Cuff = 59, Analysis = 58

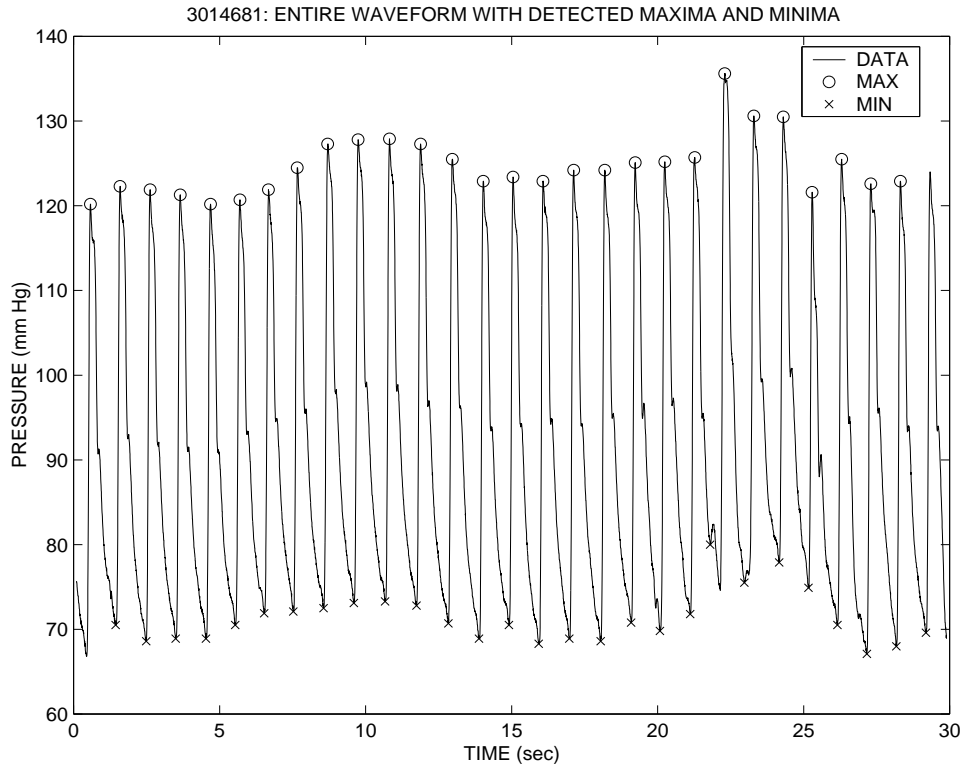
Note that in some cases, such as 7010150, the detected notch using the exponential goodness-of-fit is to the right of the “true” notch. In this case, there is evidence of two time constants to the right of the true dichrotic notch, and the single-exponential test finds the leftmost point for which a *single* exponential model is accurate.

I note that some data files are *not* processed correctly by the algorithms in their current form (I have five such files, but their analysis is not included in these notes). In some cases, the algorithm for detecting maxima and minima is unreliable. Also, in some of the cases

that are included in these notes, there may be some errors in specifying the full-cycle pulses. In some cases, the detection of maxima and minima “misses” a pulse, and this may lead to inclusion of an improper pulse in the set of similar full-cycle pulses. (This needs to be checked further.)

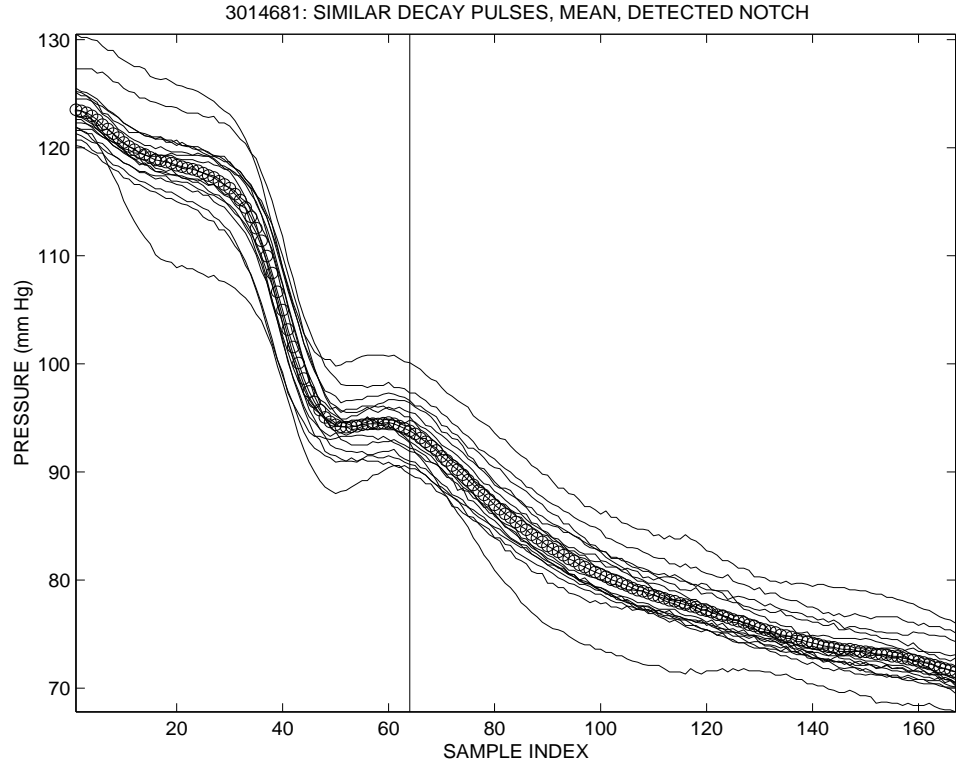


(a)

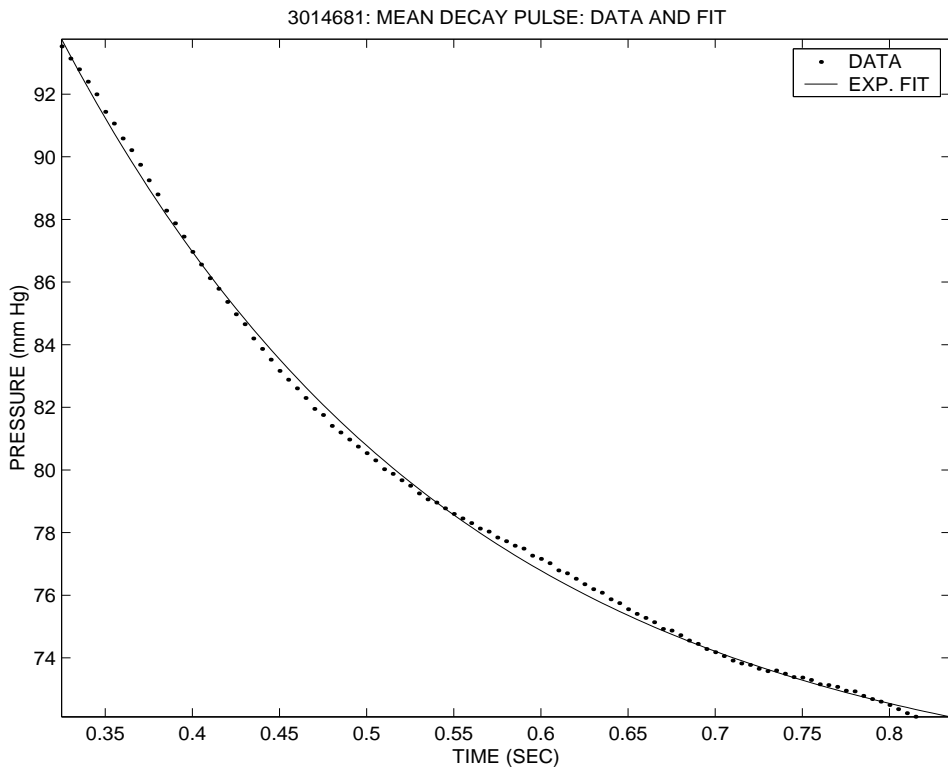


(b)

Figure 1: Data set 3014681: (a) Entire waveform and derivatives. (b) Detected maxima and minima.



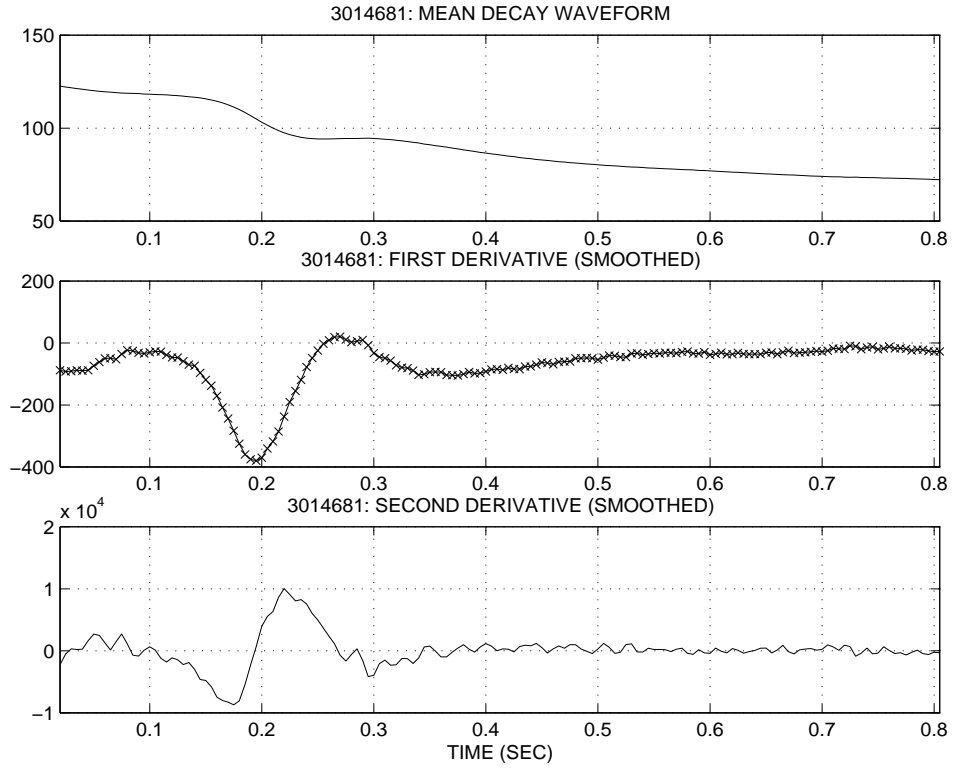
(a)



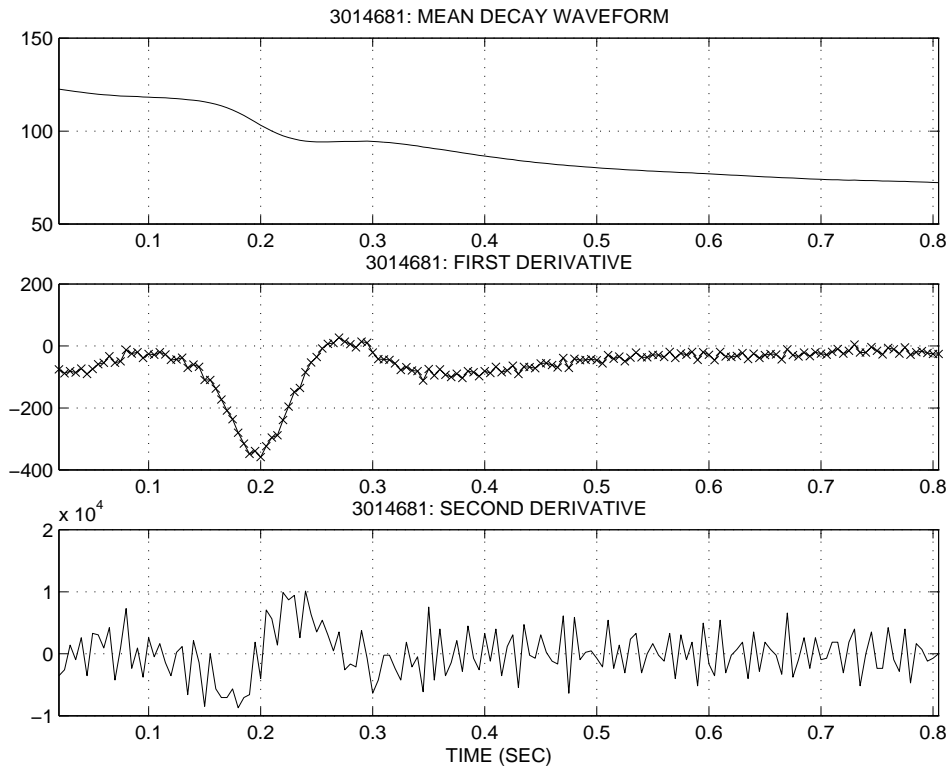
(b)

Figure 2: Data set 3014681: (a) Similar decay waveforms and mean, with detected dichrotic notch indicated by vertical line. (b) Monoexponential fit from notch to diastole.



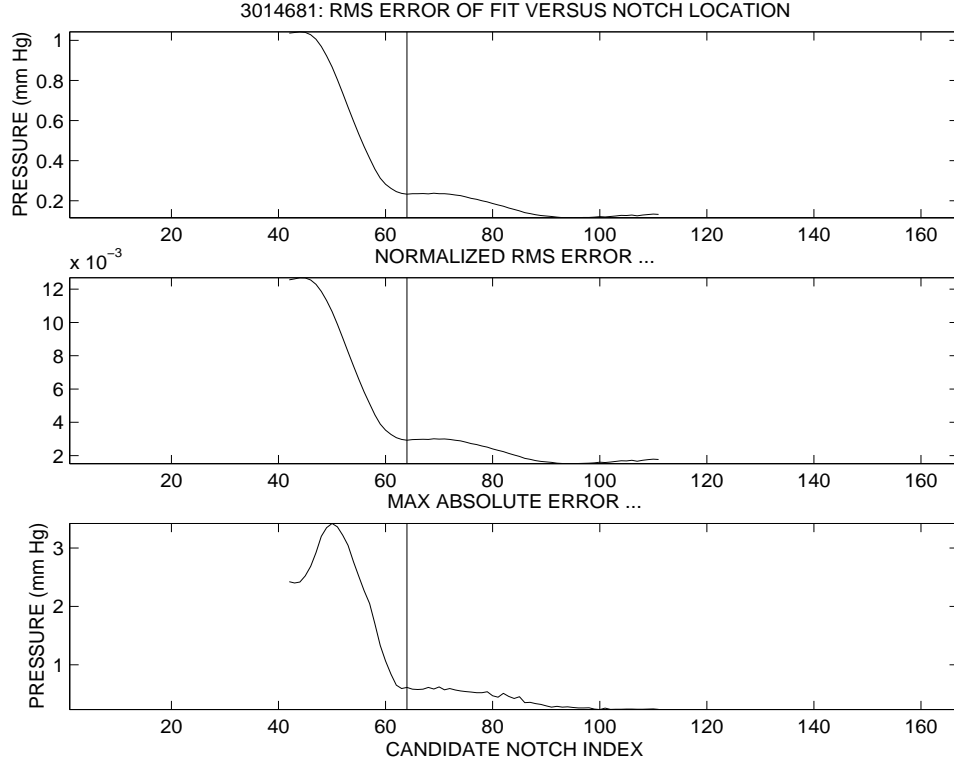


(a)

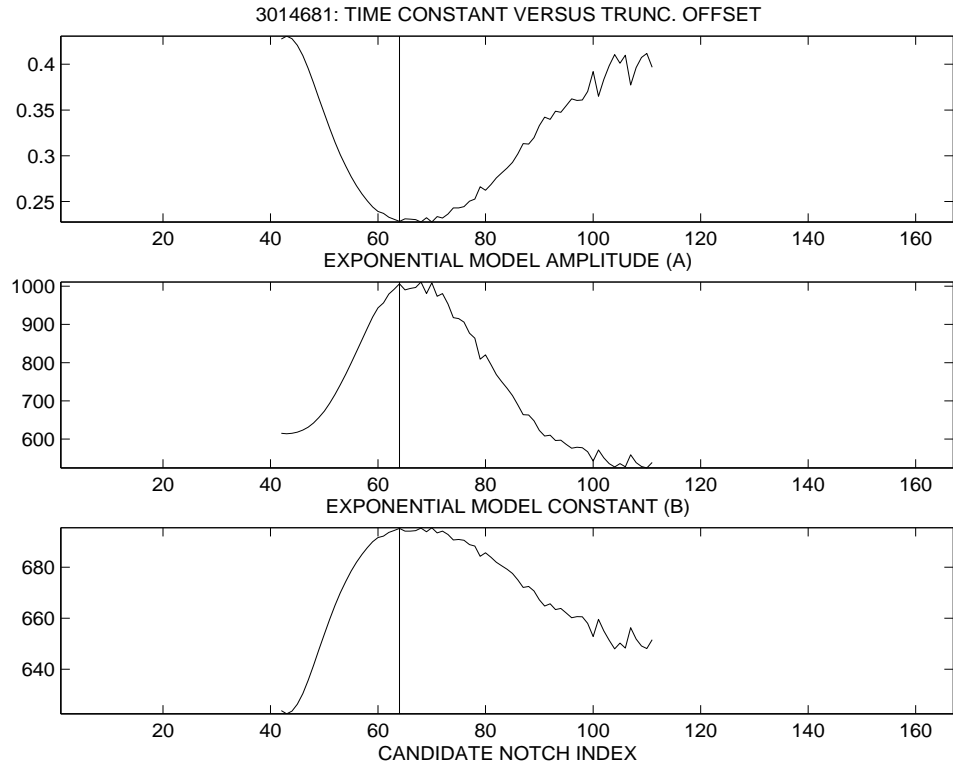


(b)

Figure 3: Data set 3014681: Mean decay waveform and derivatives (a) with and (b) without smoothing.



(a)



(b)

Figure 4: Data set 3014681: (a) Goodness-of-fit measures to exponential model for different choices of dichrotic notch location. (b) Variation in exponential model parameters for different choices of dichrotic notch location.

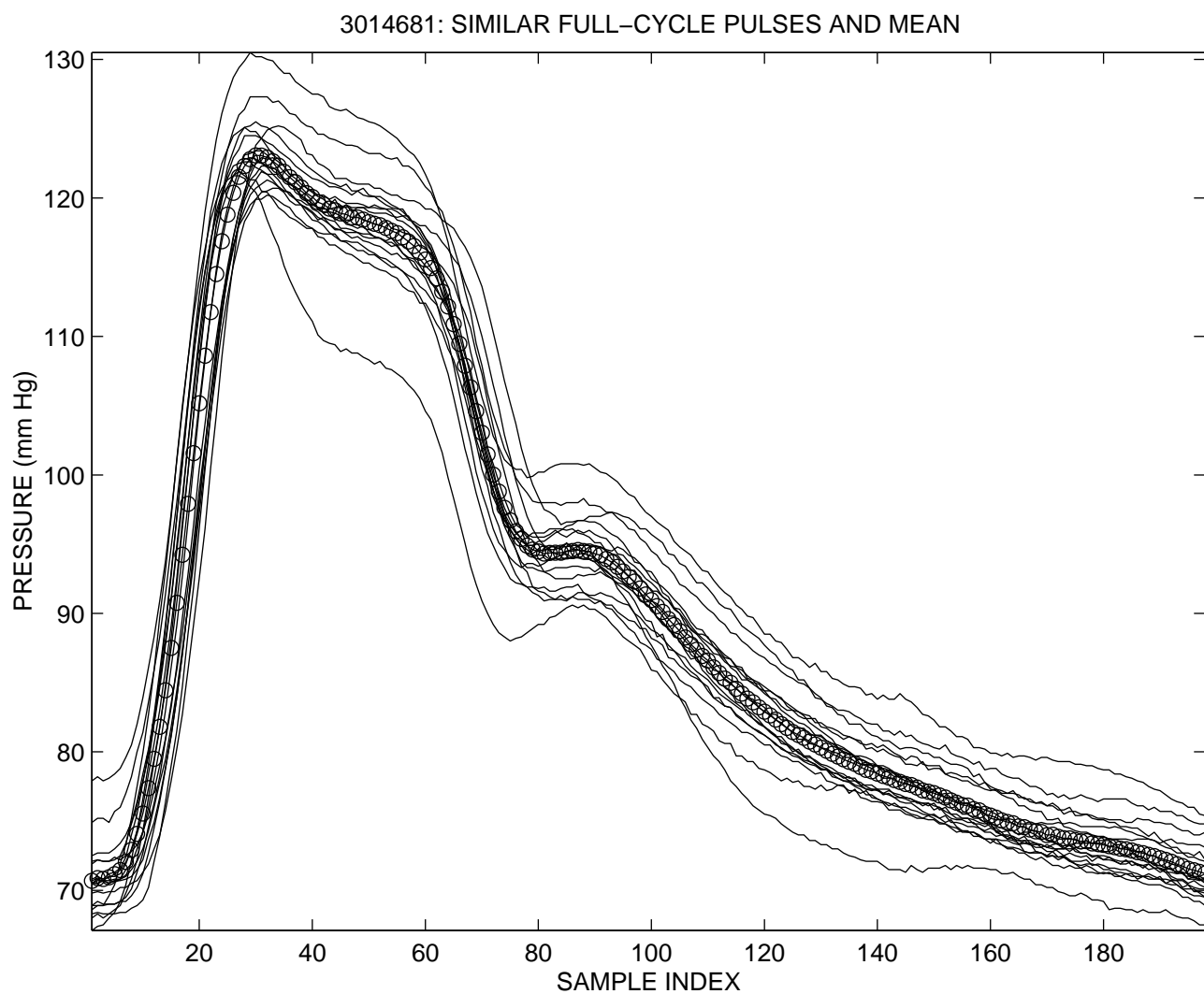


Figure 5: Data set 3014681: Similar full-cycle pulses and mean.

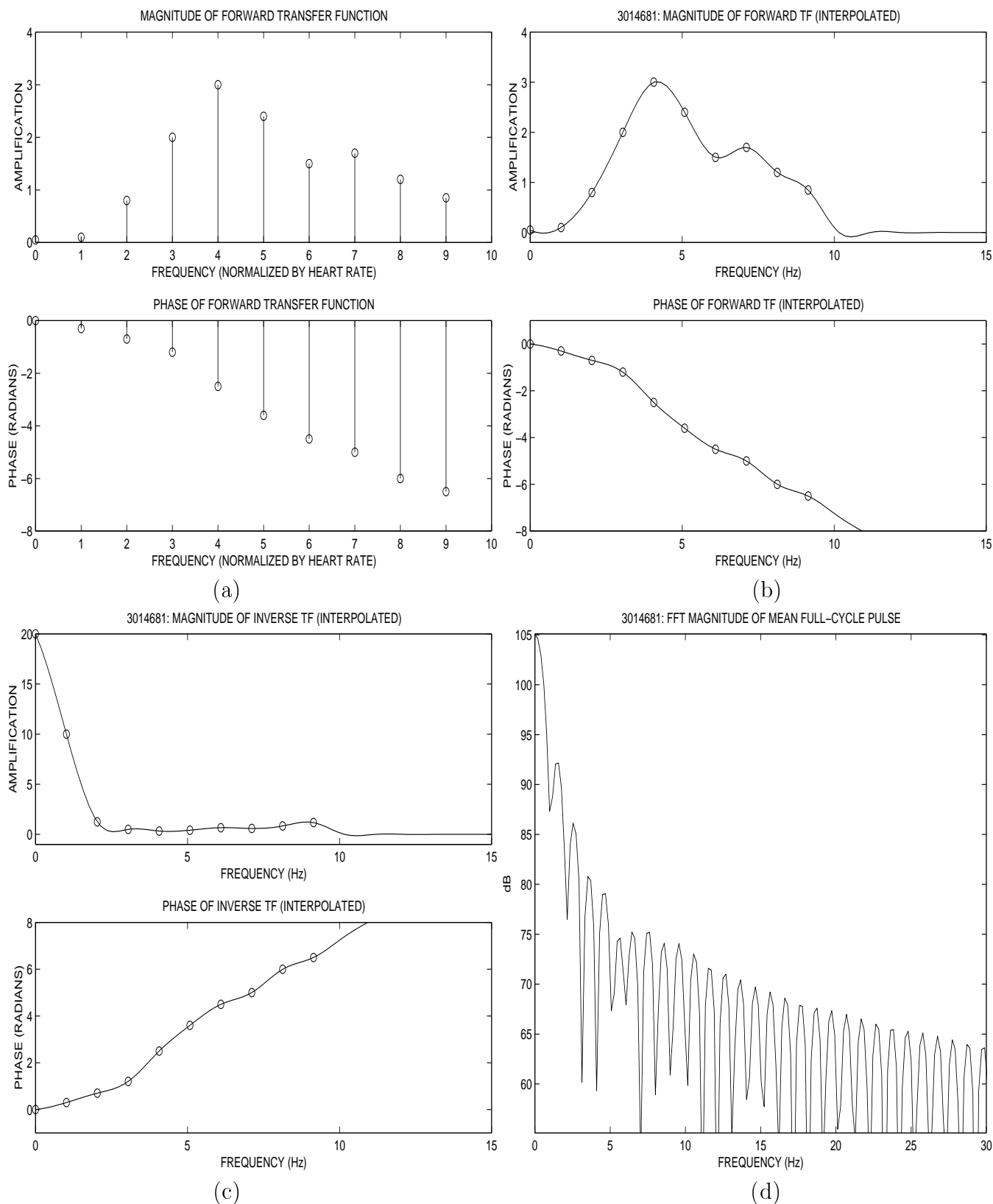
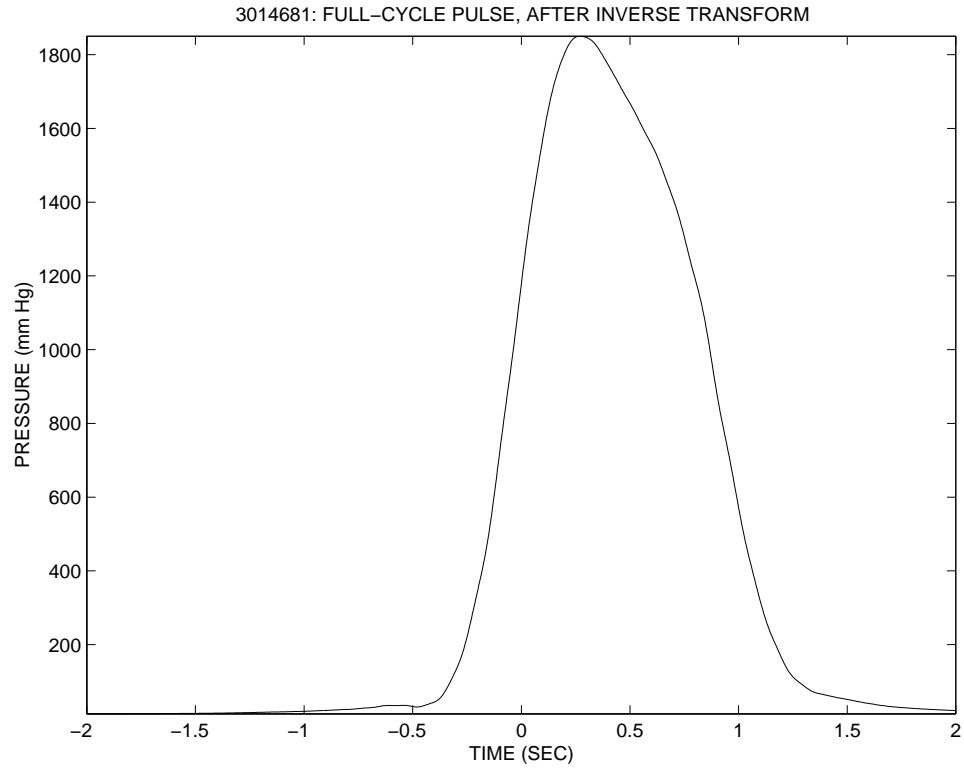
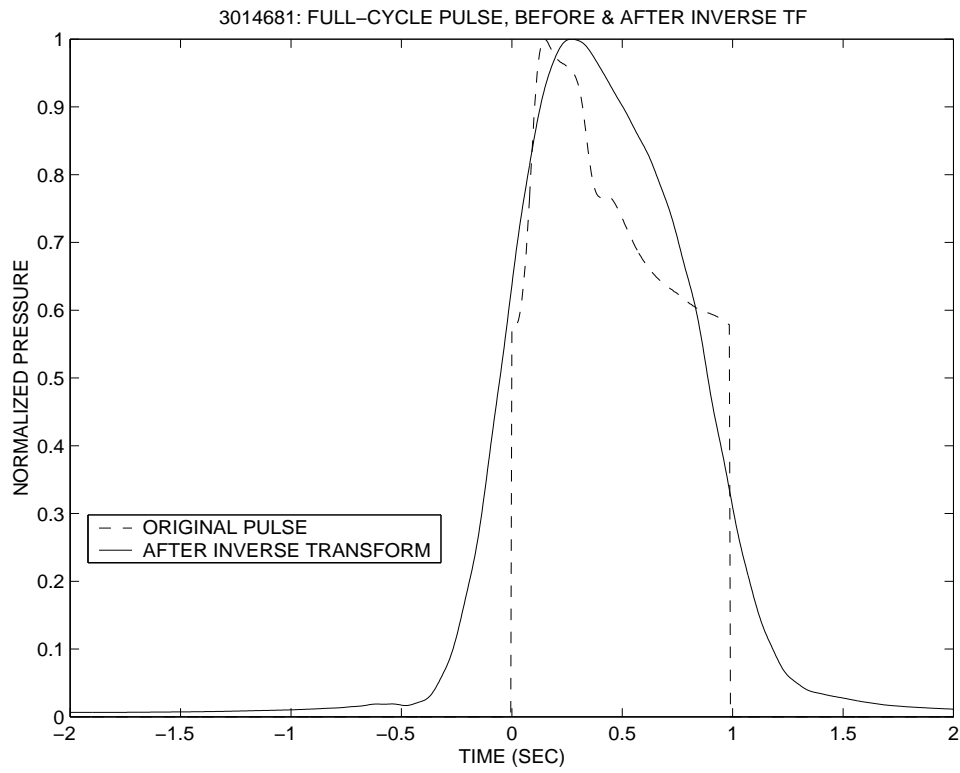


Figure 6: Data set 3014681: (a) Estimate of forward TF, from published graph. (b) Cubic-spline interpolated forward TF. (c) Cubic-spline interpolated inverse TF, with zero gain beyond ninth harmonic. (d) FFT magnitude of mean full-cycle pulse.



(a)



(b)

Figure 7: Data set 3014681: (a) Result of passing mean full-cycle pulse through inverse TF. (b) Full-cycle pulse before and after inverse transform, with peak pressure normalized to 1.

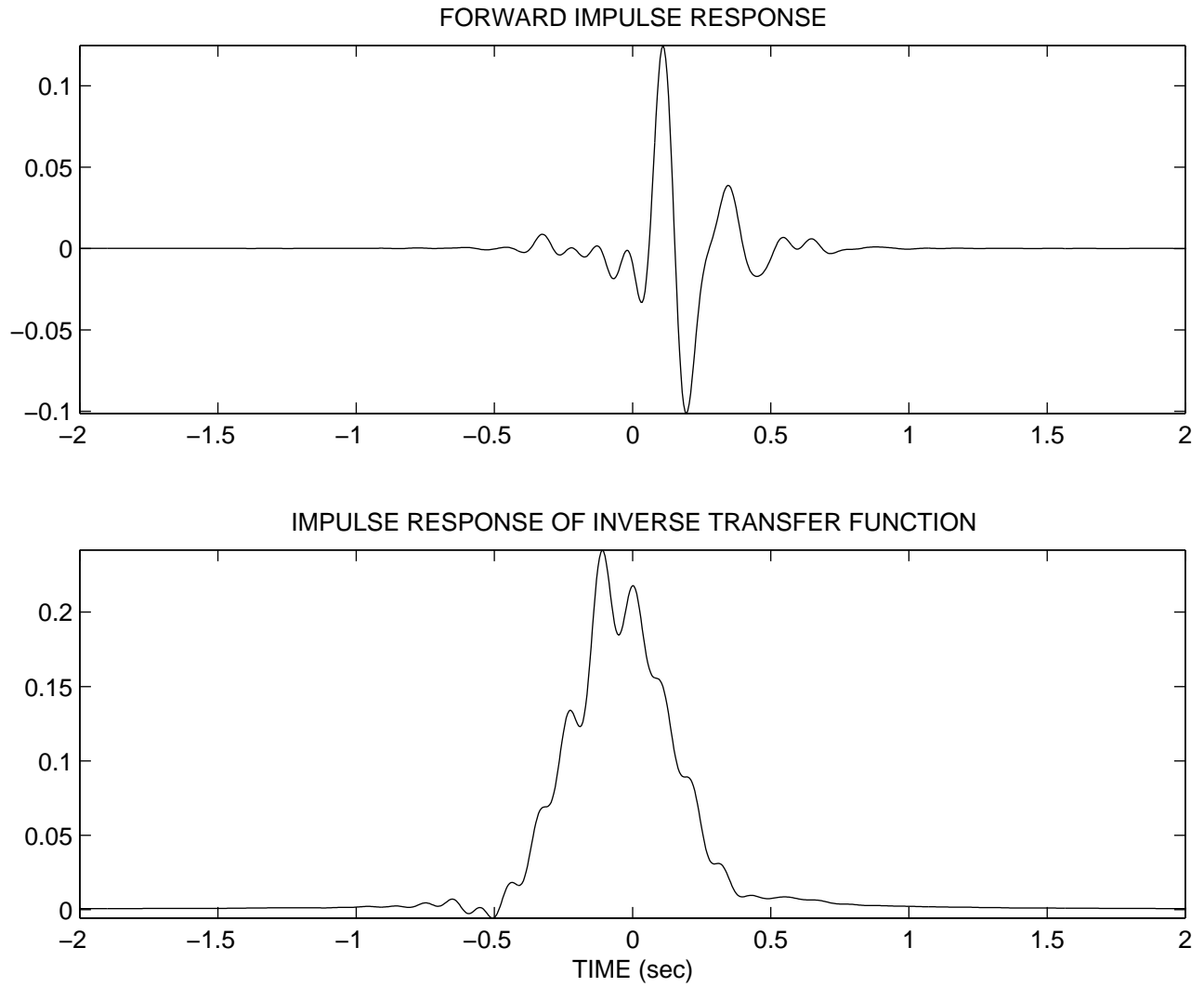
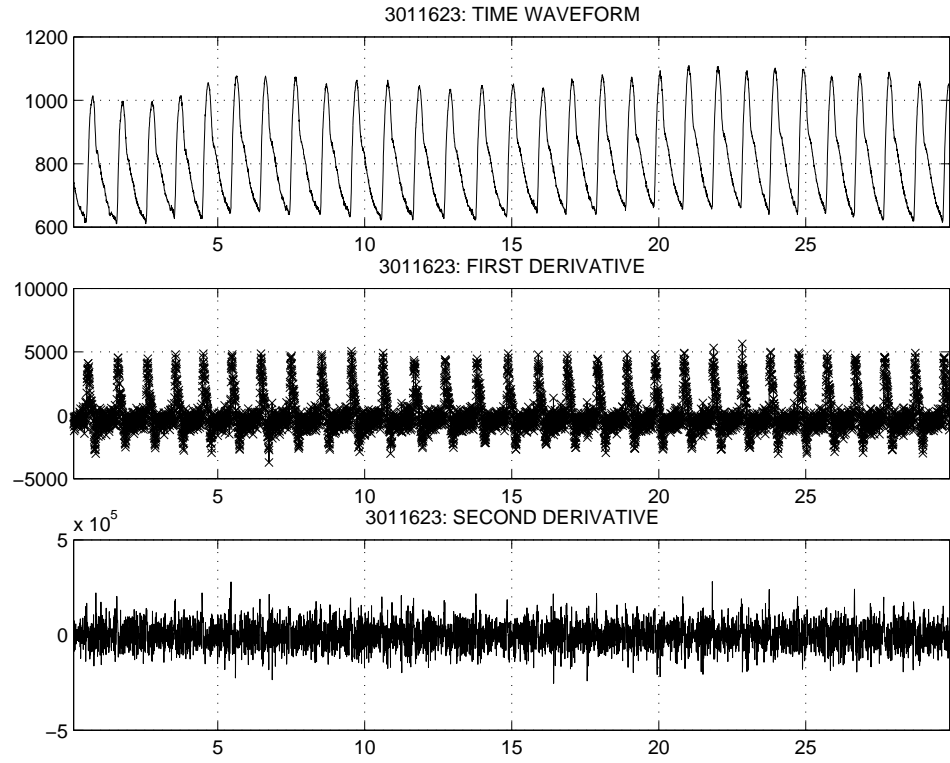
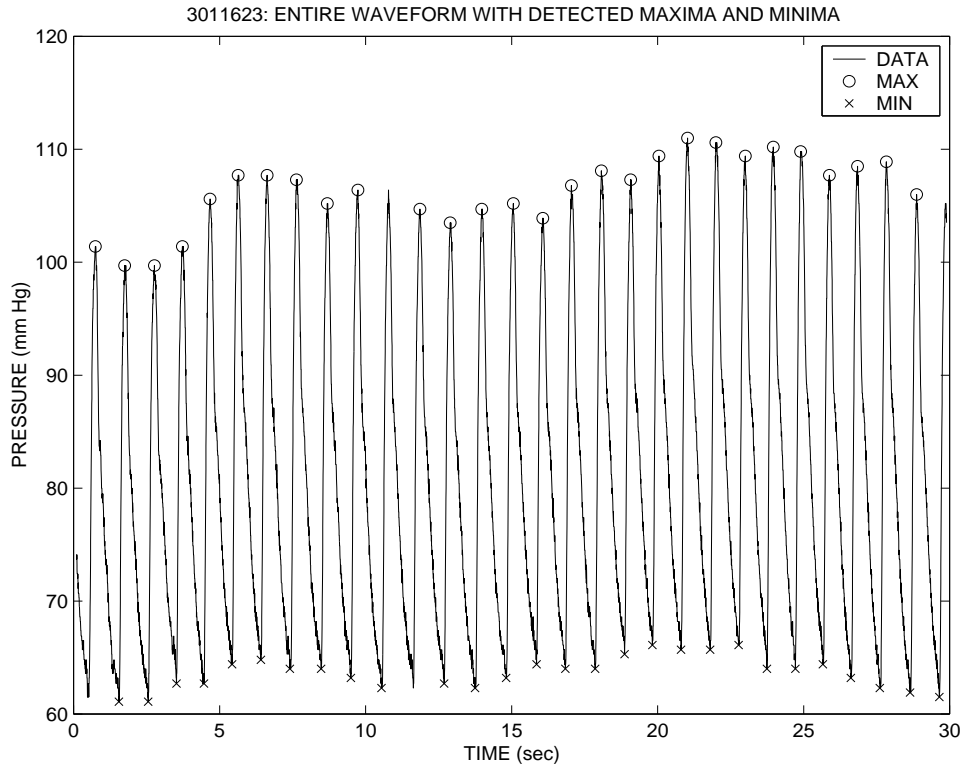


Figure 8: Data set 3014681: Impulse responses of forward and inverse TFs. The convolution of these two impulse responses resembles an impulse, as it should since these are inverses of each other.

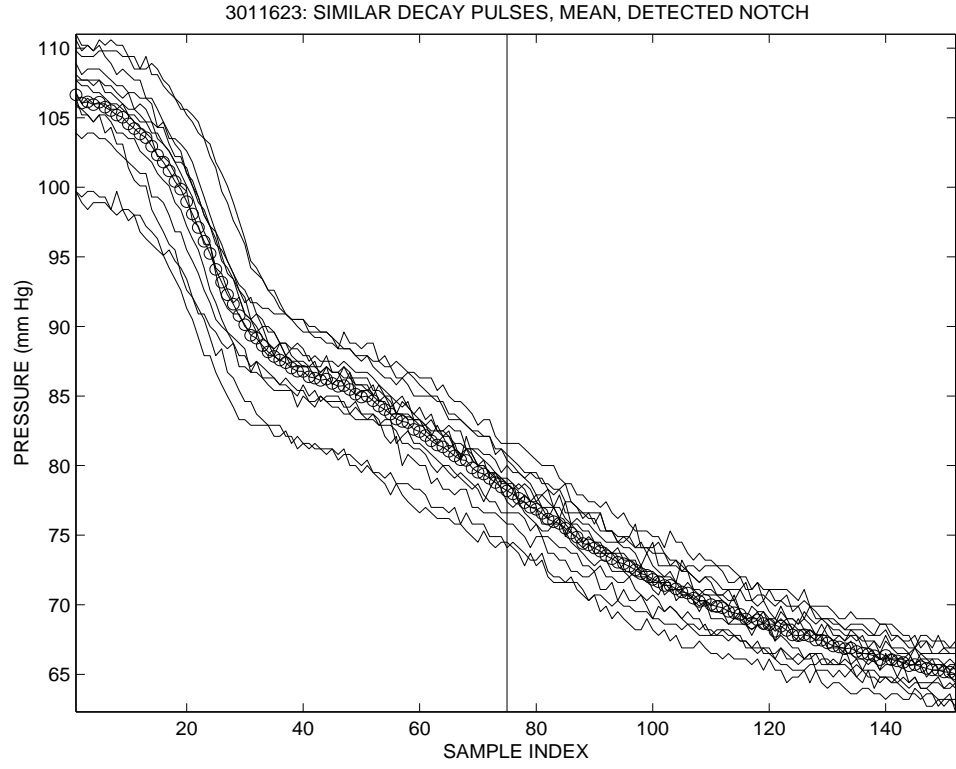


(a)

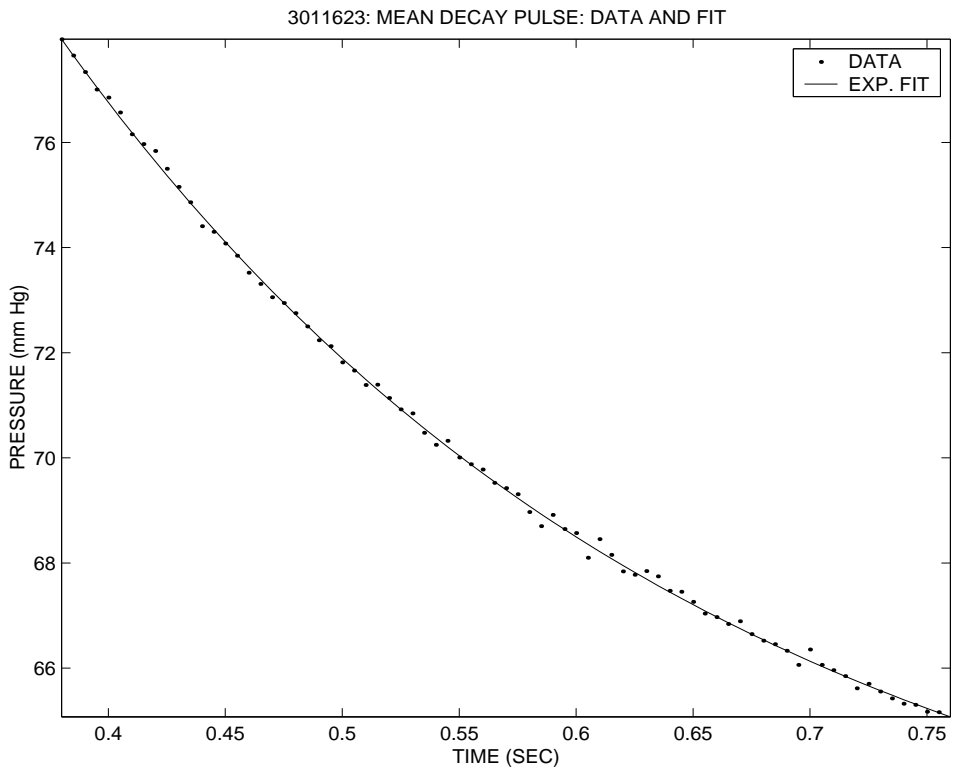


(b)

Figure 9: Data set 3011623: (a) Entire waveform and derivatives. (b) Detected maxima and minima.



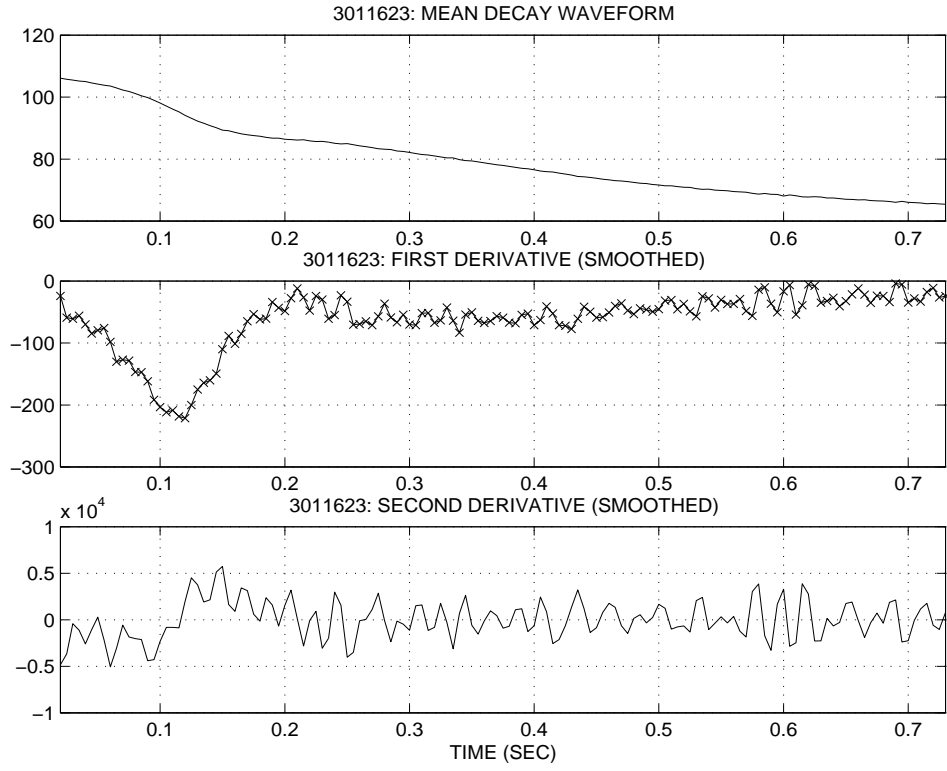
(a)



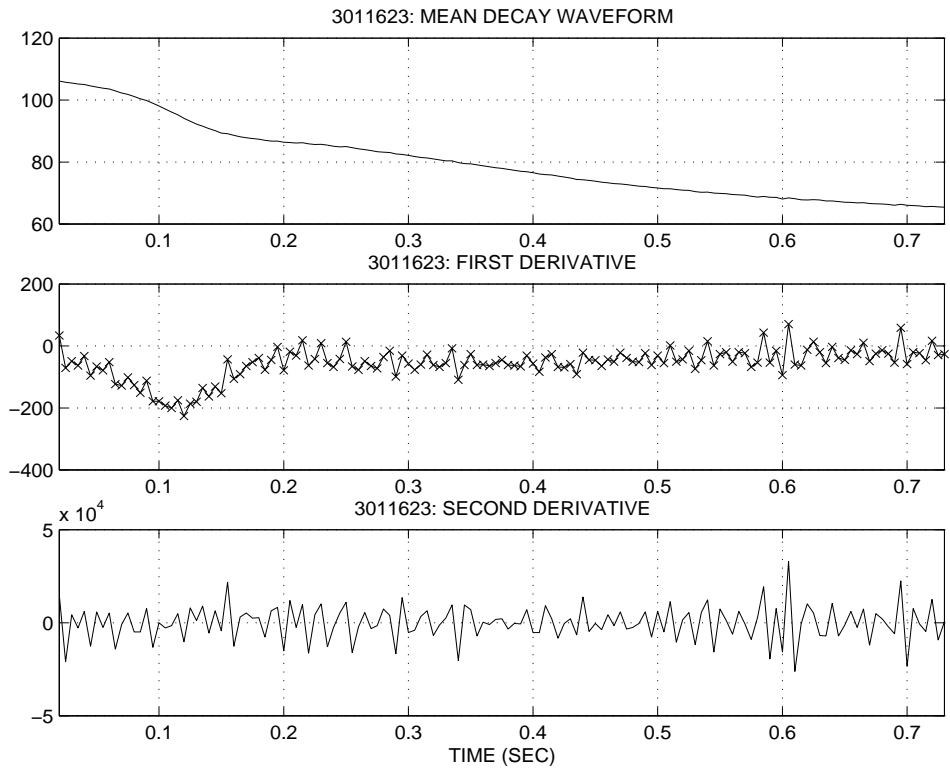
(b)

Figure 10: Data set 3011623: (a) Similar decay waveforms and mean, with detected dichrotic notch indicated by vertical line. (b) Monoexponential fit from notch to diastole.



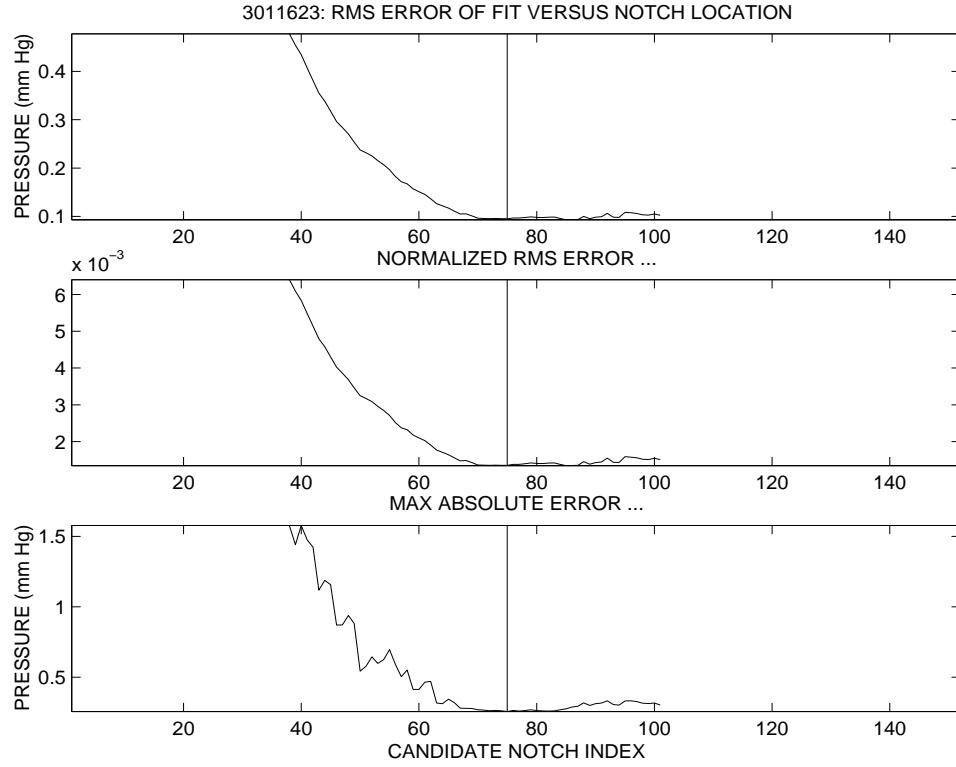


(a)

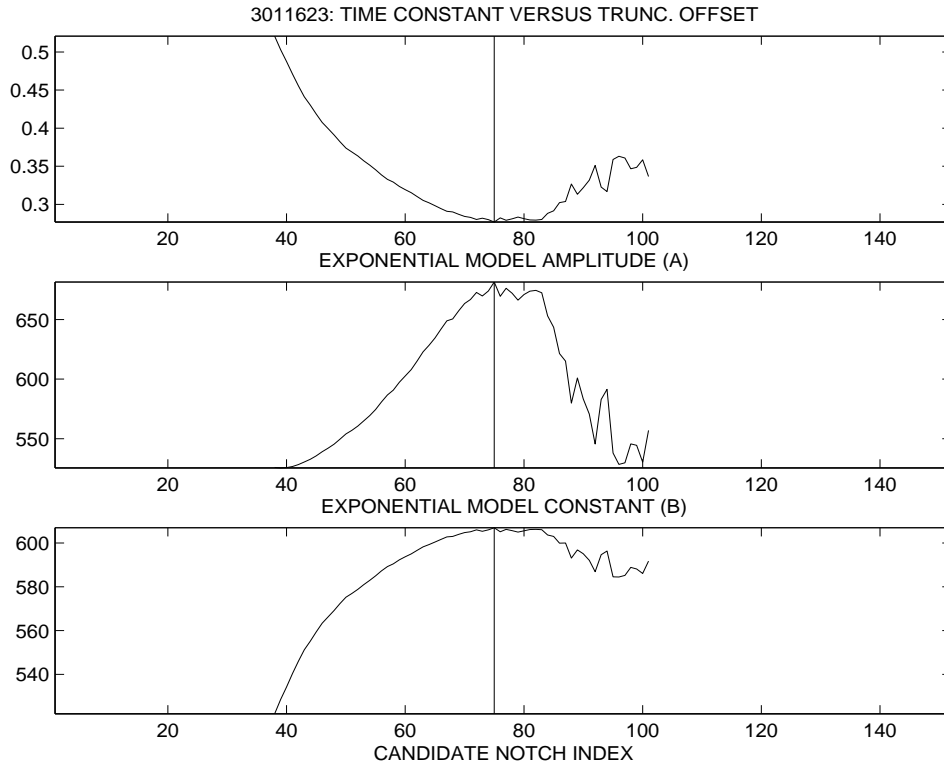


(b)

Figure 11: Data set 3011623: Mean decay waveform and derivatives (a) with and (b) without smoothing.



(a)



(b)

Figure 12: Data set 3011623: (a) Goodness-of-fit measures to exponential model for different choices of dichrotic notch location. (b) Variation in exponential model parameters for different choices of dichrotic notch location.

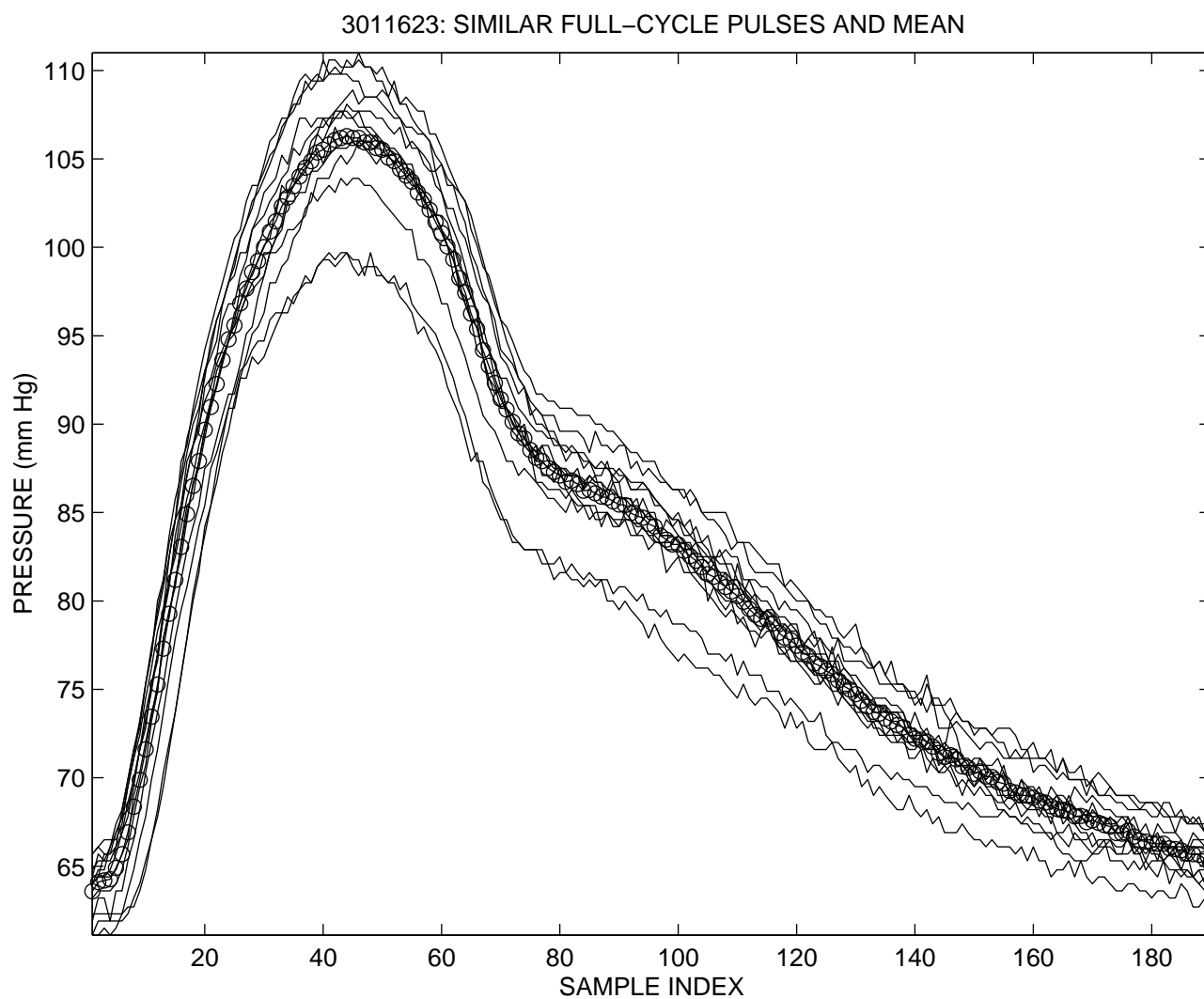


Figure 13: Data set 3011623: Similar full-cycle pulses and mean.

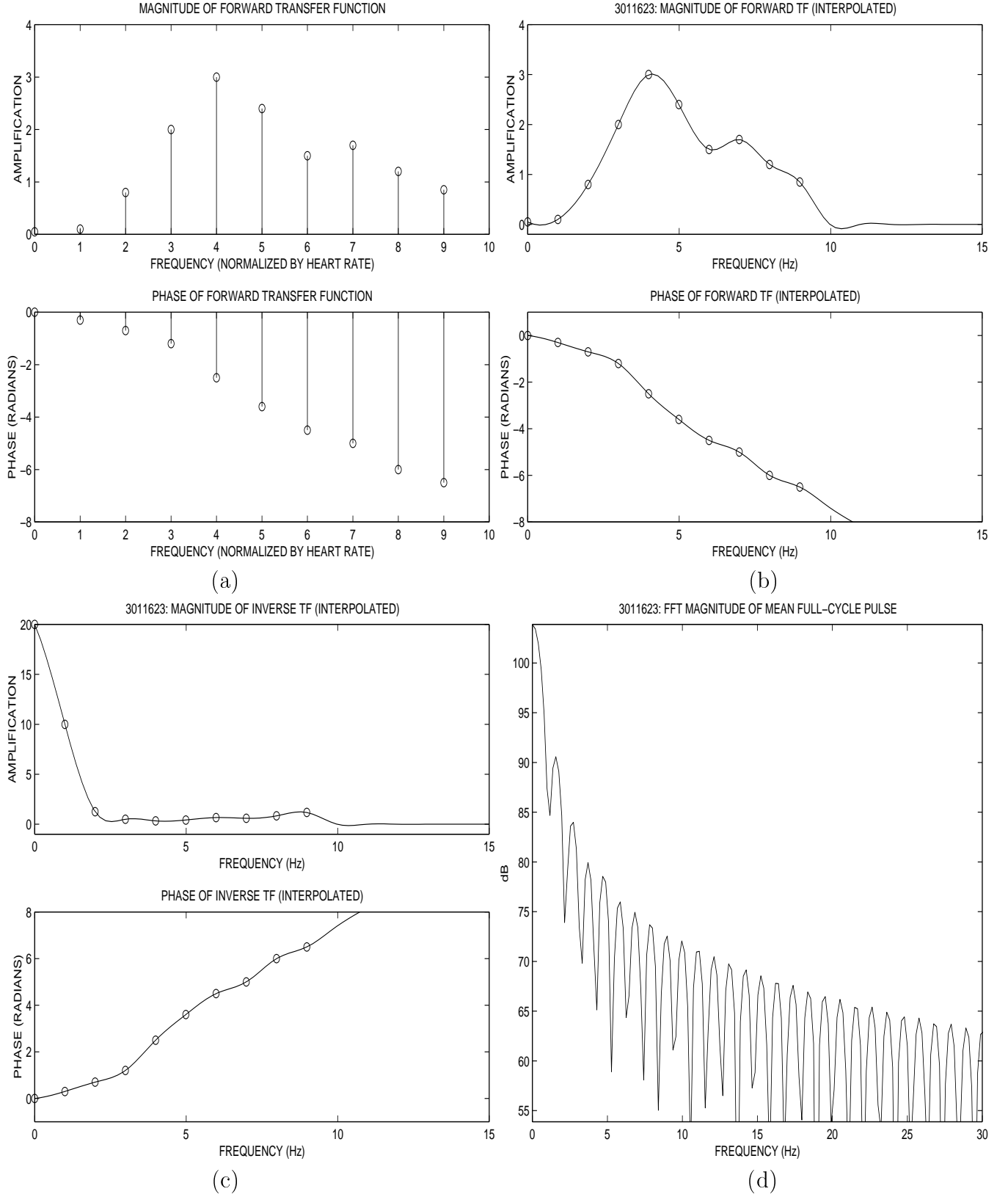
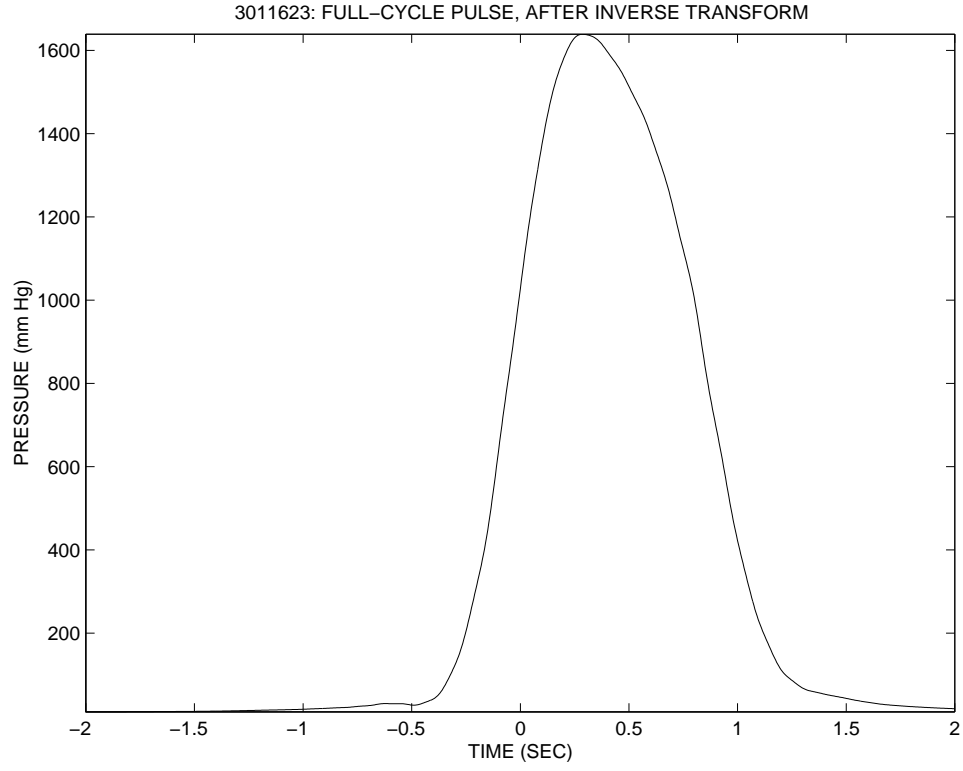
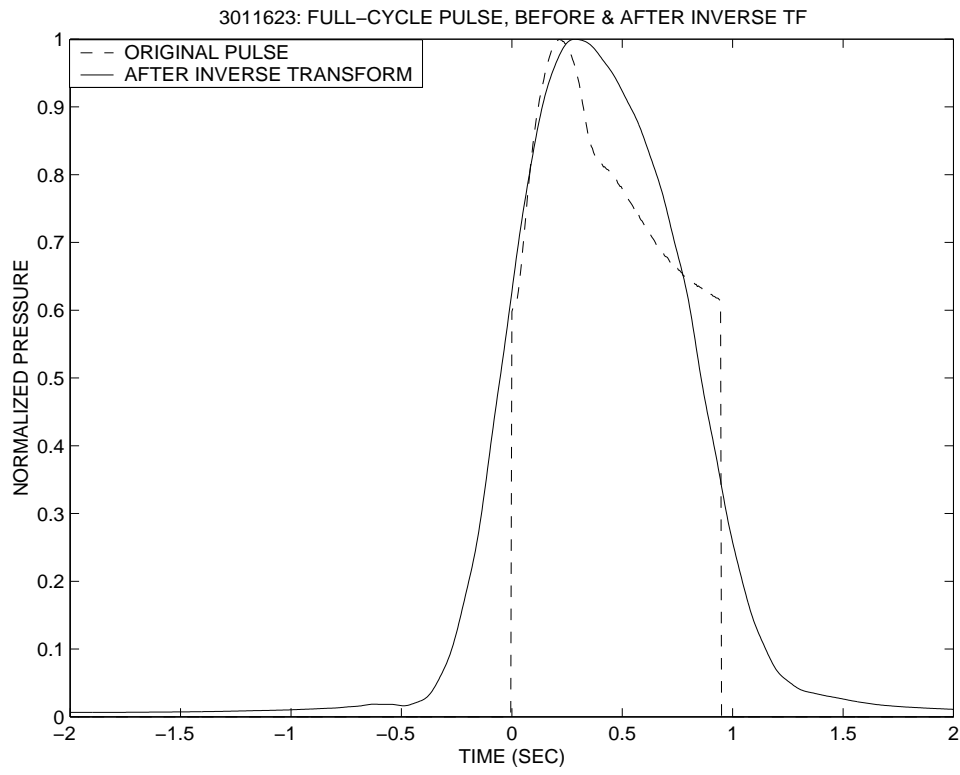


Figure 14: Data set 3011623: (a) Estimate of forward TF, from published graph. (b) Cubic-spline interpolated forward TF. (c) Cubic-spline interpolated inverse TF, with zero gain beyond ninth harmonic. (d) FFT magnitude of mean full-cycle pulse.

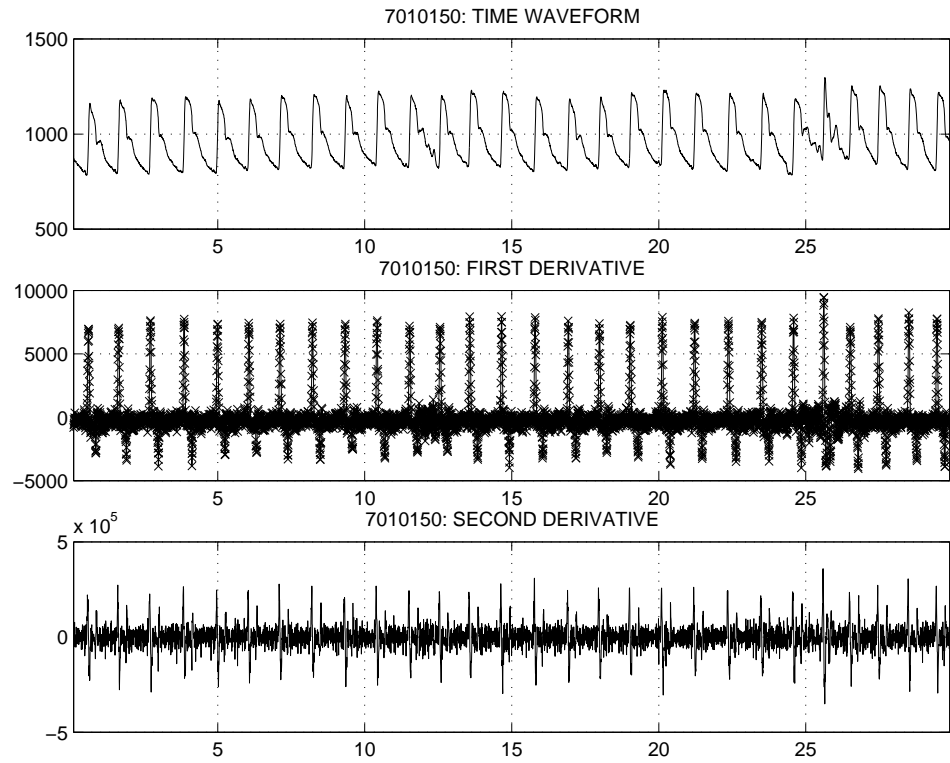


(a)

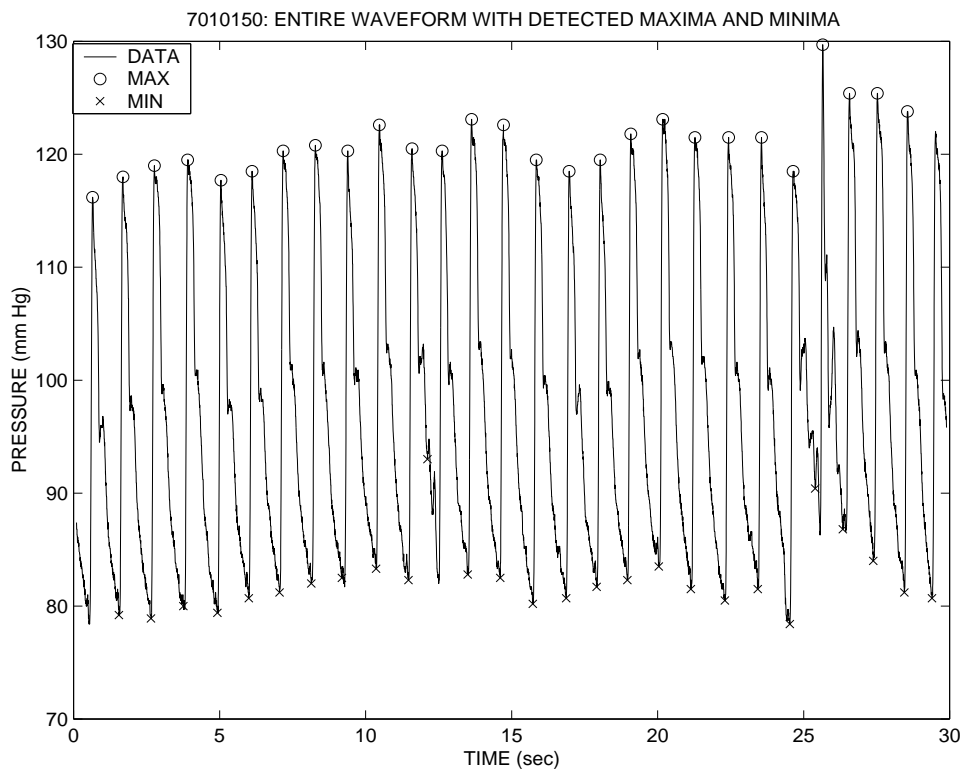


(b)

Figure 15: Data set 3011623: (a) Result of passing mean full-cycle pulse through inverse TF. (b) Full-cycle pulse before and after inverse transform, with peak pressure normalized to 1.

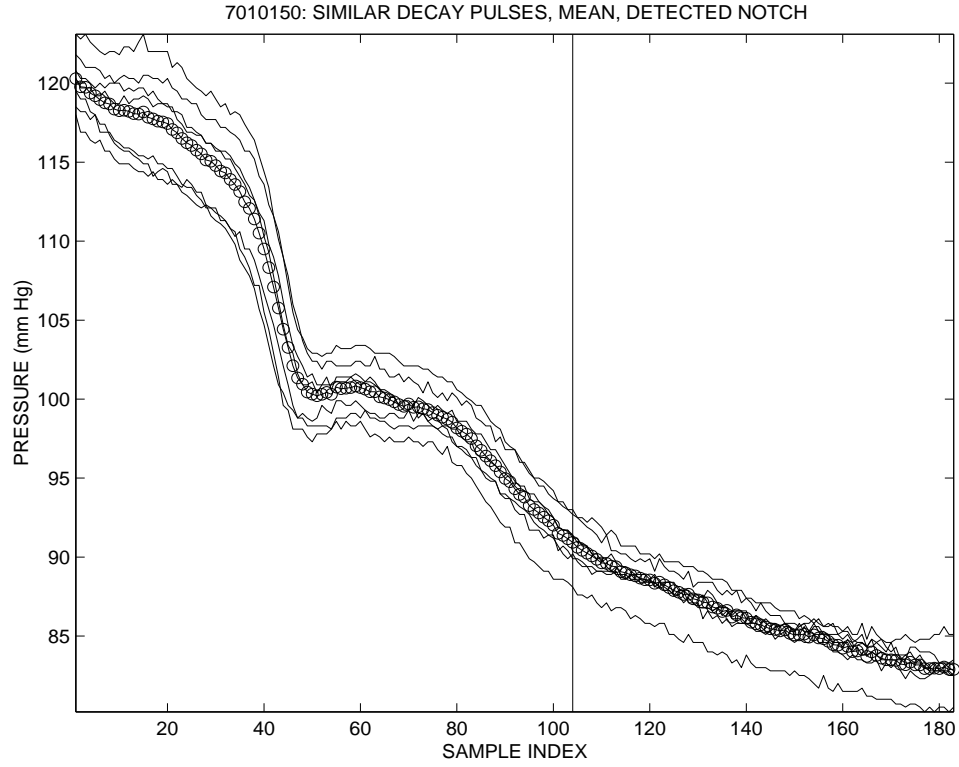


(a)

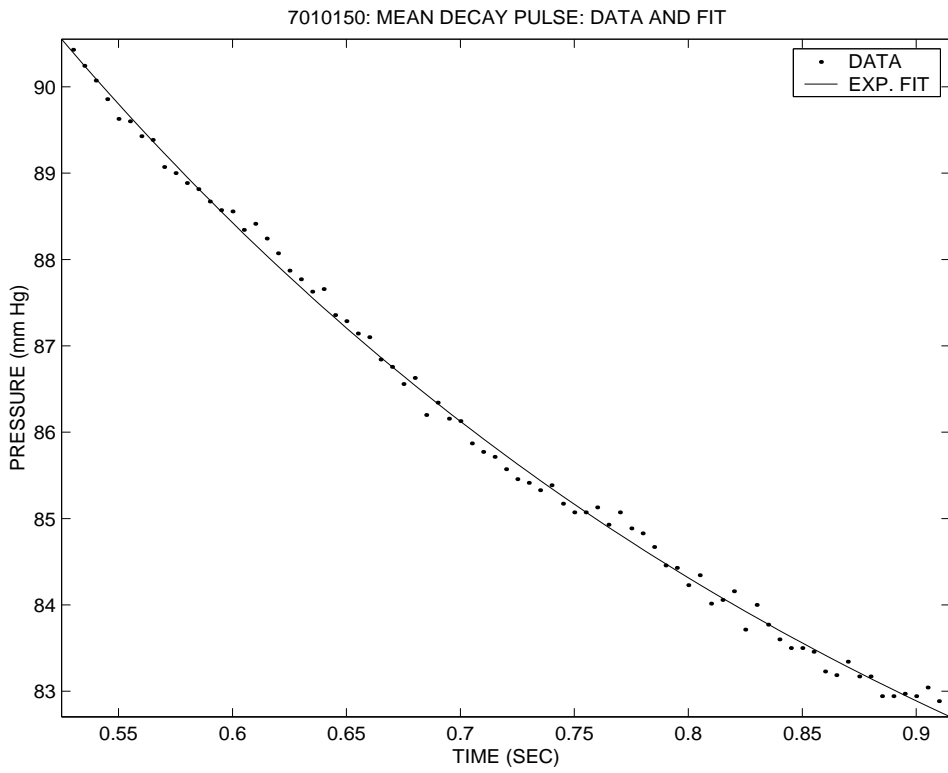


(b)

Figure 16: Data set 7010150: (a) Entire waveform and derivatives. (b) Detected maxima and minima.

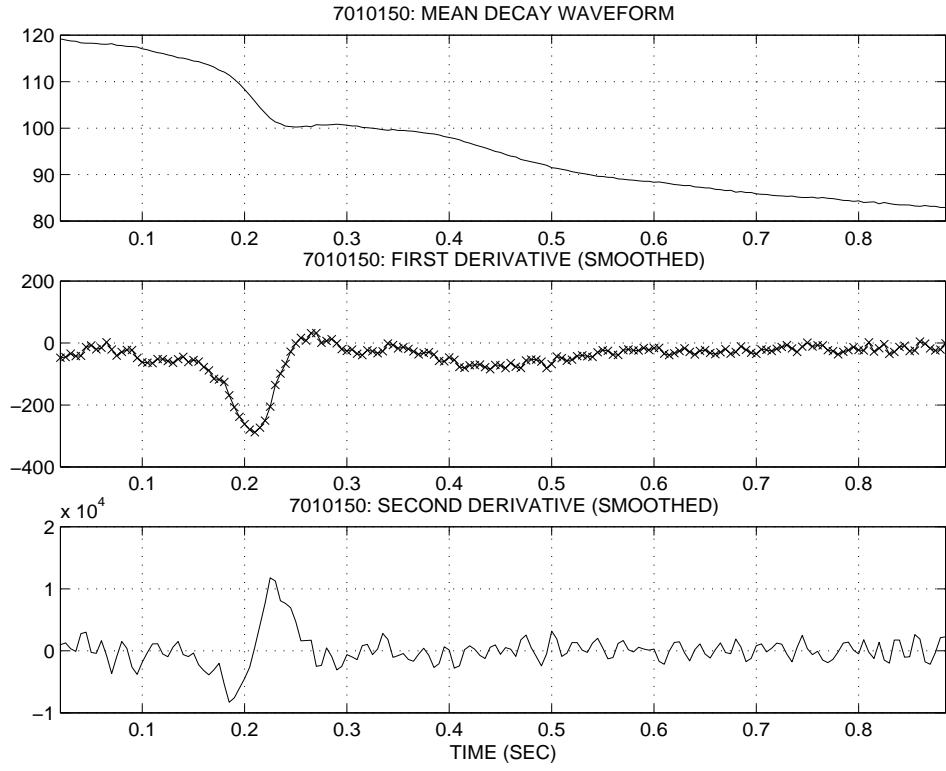


(a)

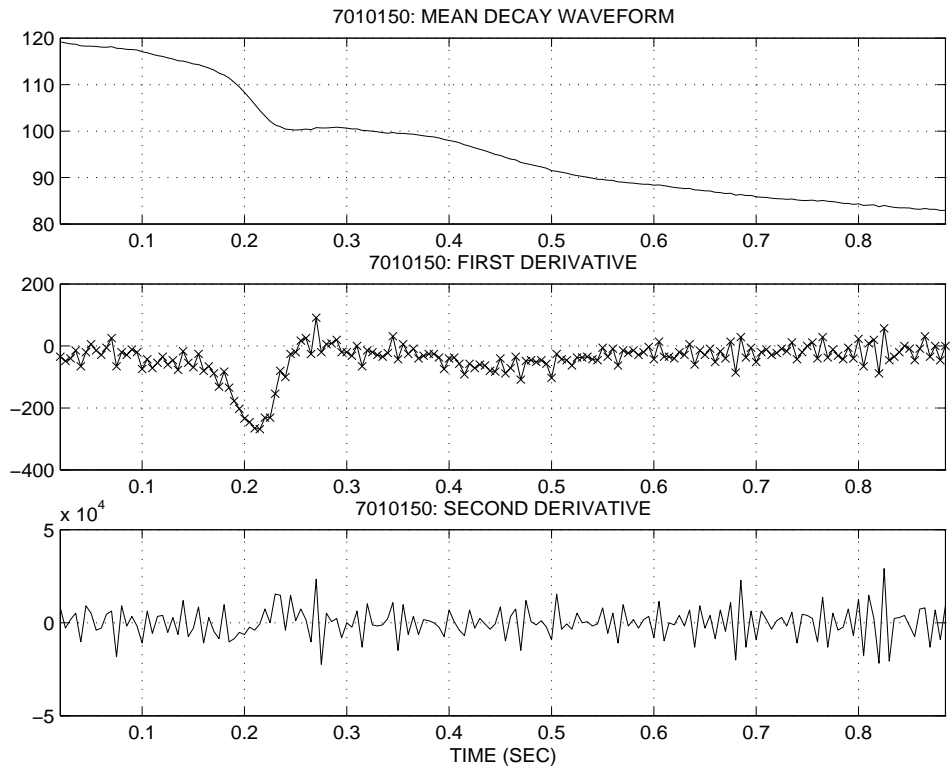


(b)

Figure 17: Data set 7010150: (a) Similar decay waveforms and mean, with detected dichrotic notch indicated by vertical line. (b) Monoexponential fit from notch to diastole.



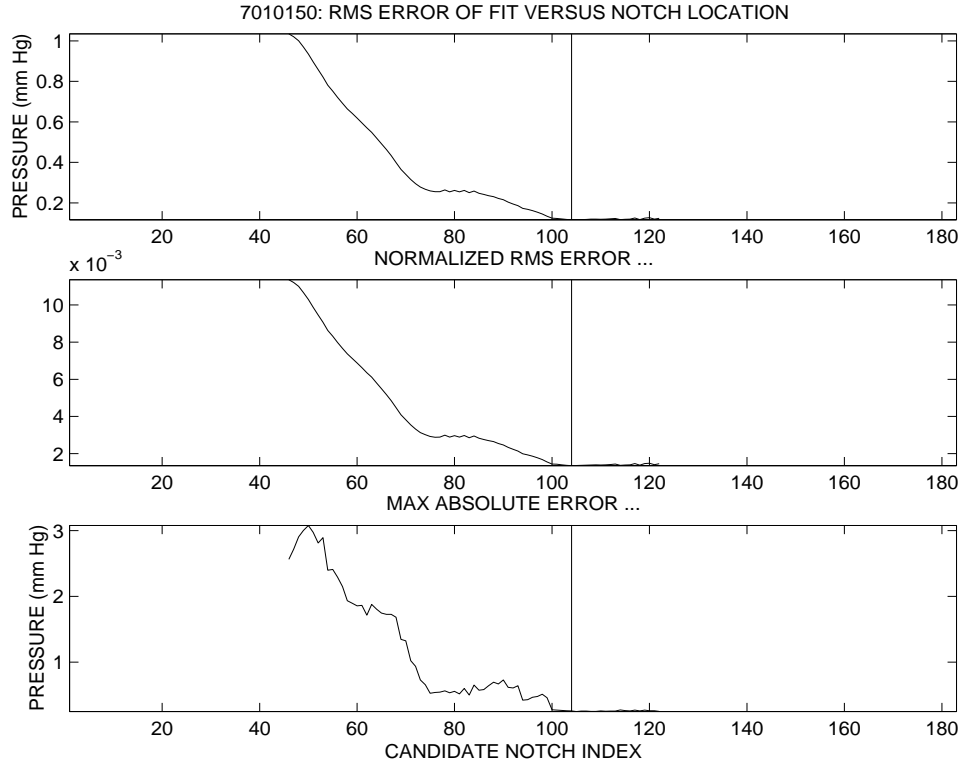
(a)



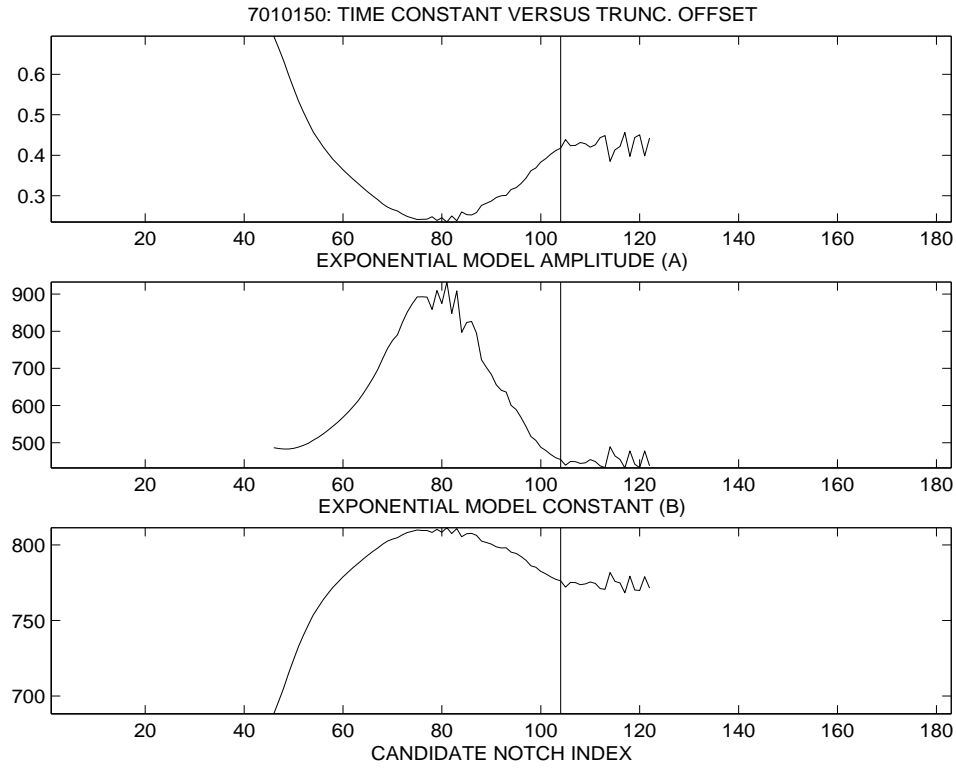
(b)

Figure 18: Data set 7010150: Mean decay waveform and derivatives (a) with and (b) without smoothing.





(a)



(b)

Figure 19: Data set 7010150: (a) Goodness-of-fit measures to exponential model for different choices of dichrotic notch location. (b) Variation in exponential model parameters for different choices of dichrotic notch location.

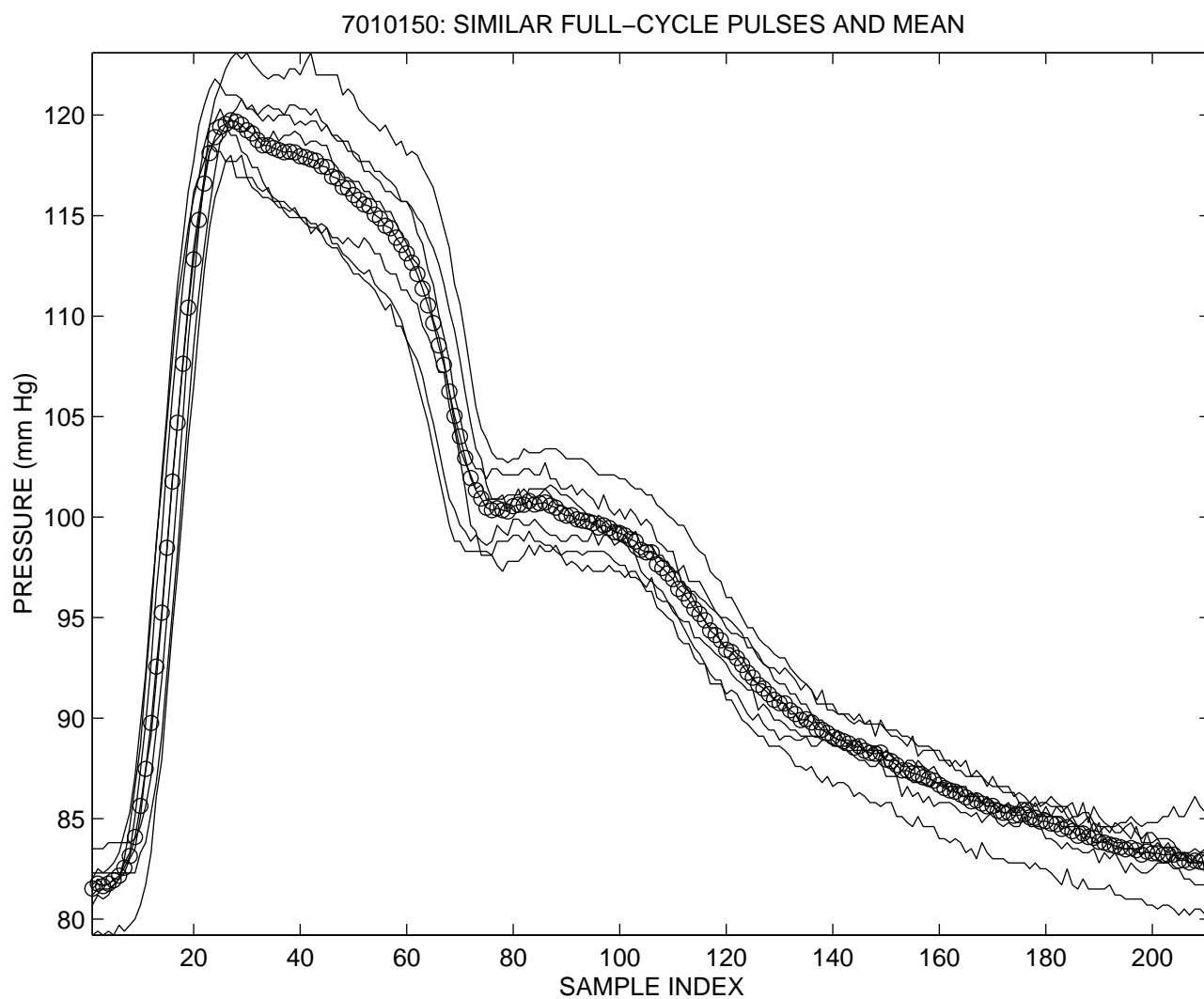


Figure 20: Data set 7010150: Similar full-cycle pulses and mean.

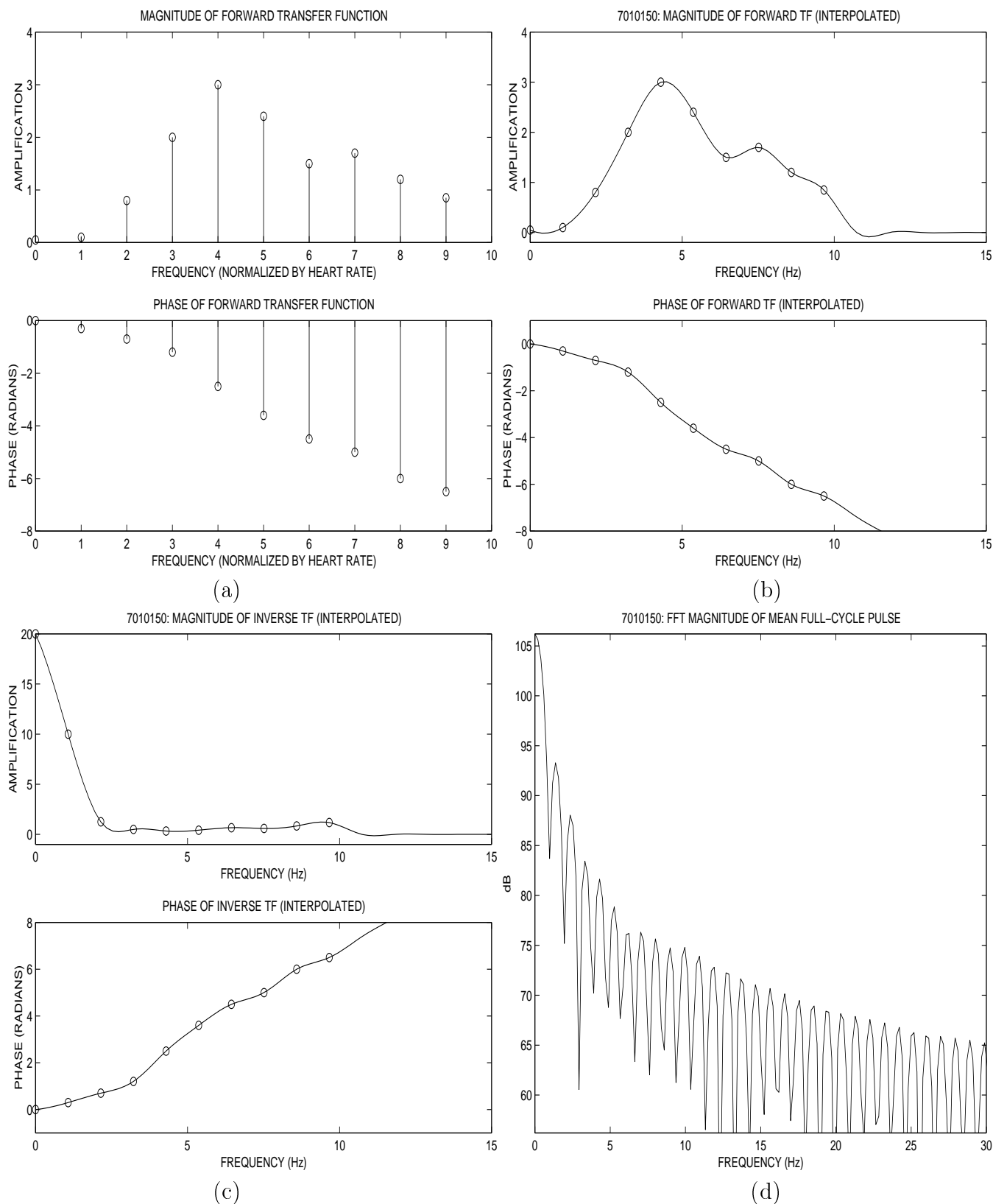
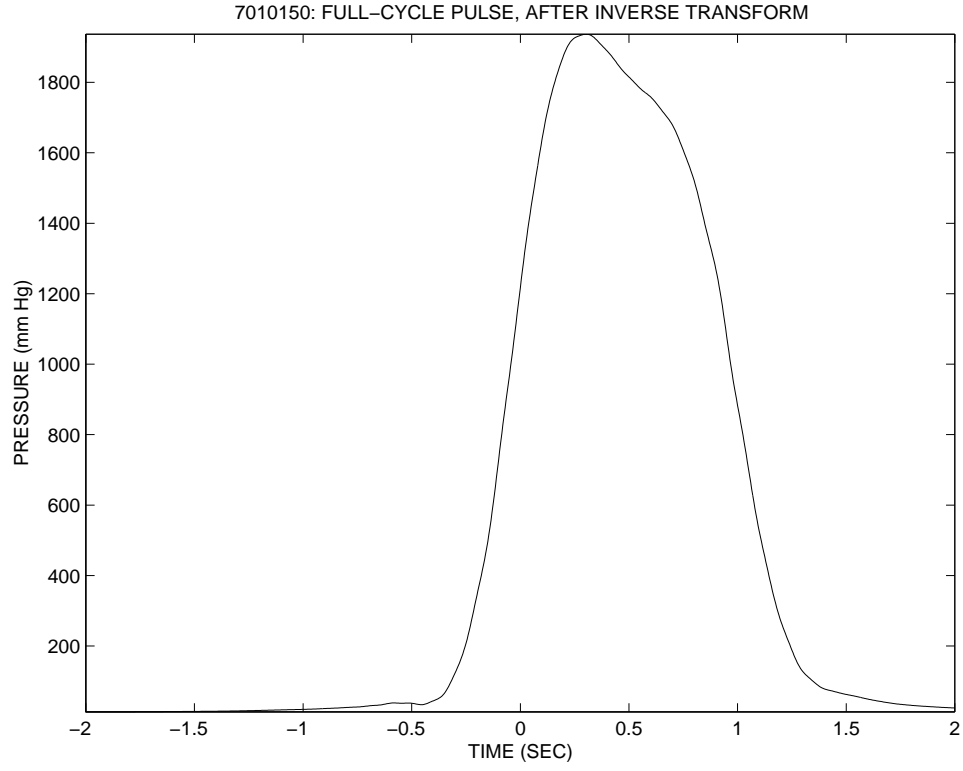
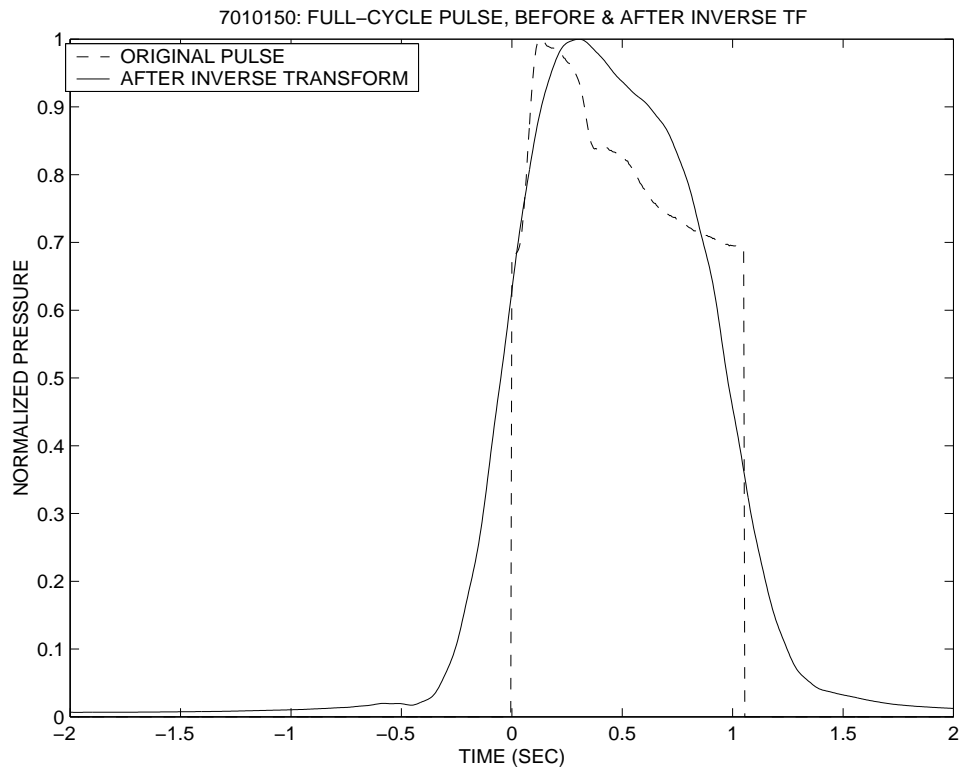


Figure 21: Data set 7010150: (a) Estimate of forward TF, from published graph. (b) Cubic-spline interpolated forward TF. (c) Cubic-spline interpolated inverse TF, with zero gain beyond ninth harmonic. (d) FFT magnitude of mean full-cycle pulse.

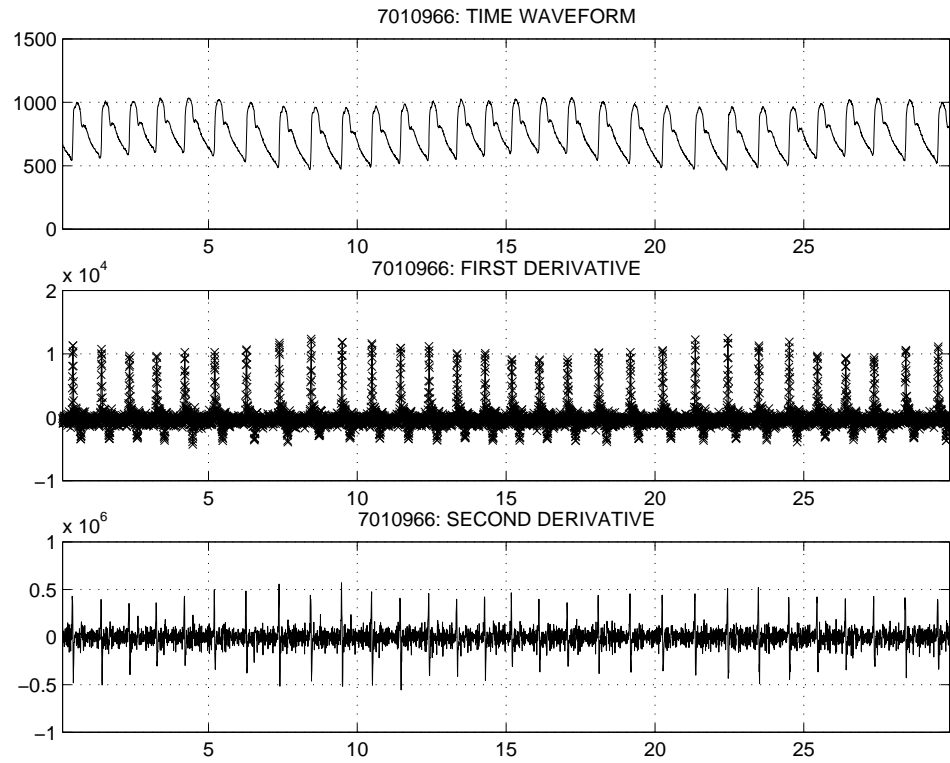


(a)

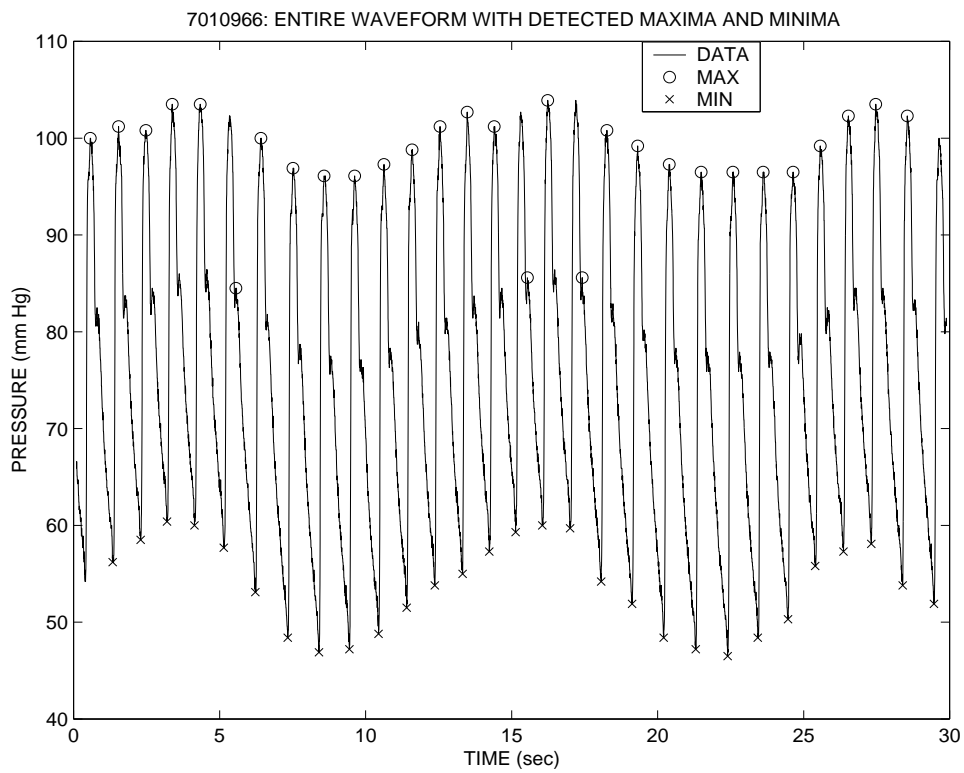


(b)

Figure 22: Data set 7010150: (a) Result of passing mean full-cycle pulse through inverse TF. (b) Full-cycle pulse before and after inverse transform, with peak pressure normalized to 1.

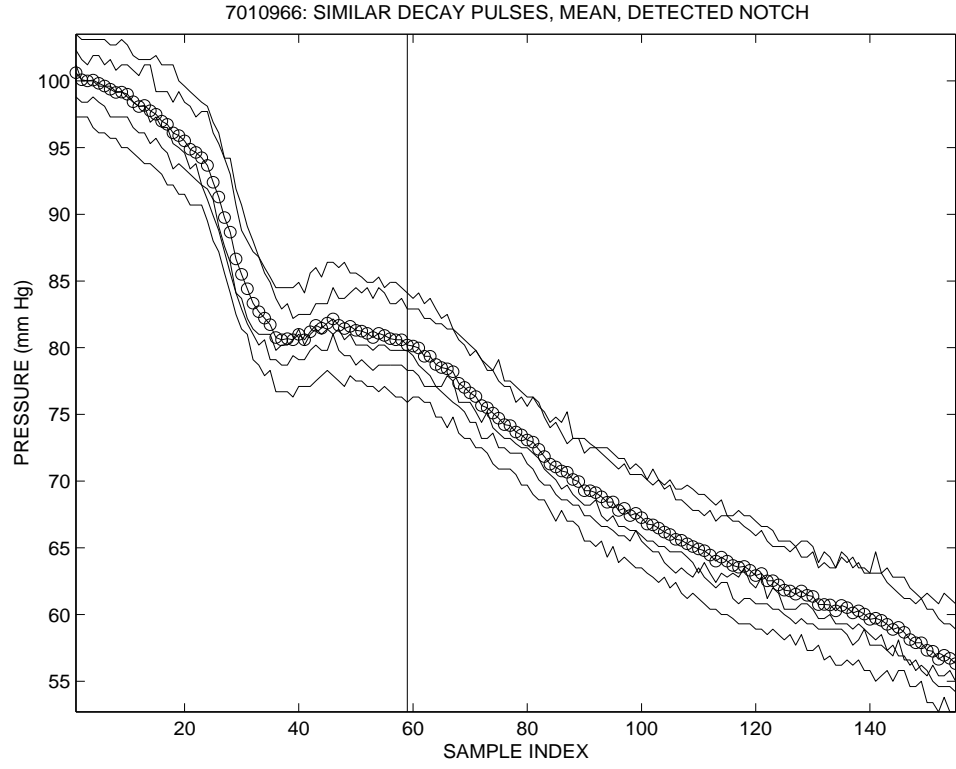


(a)

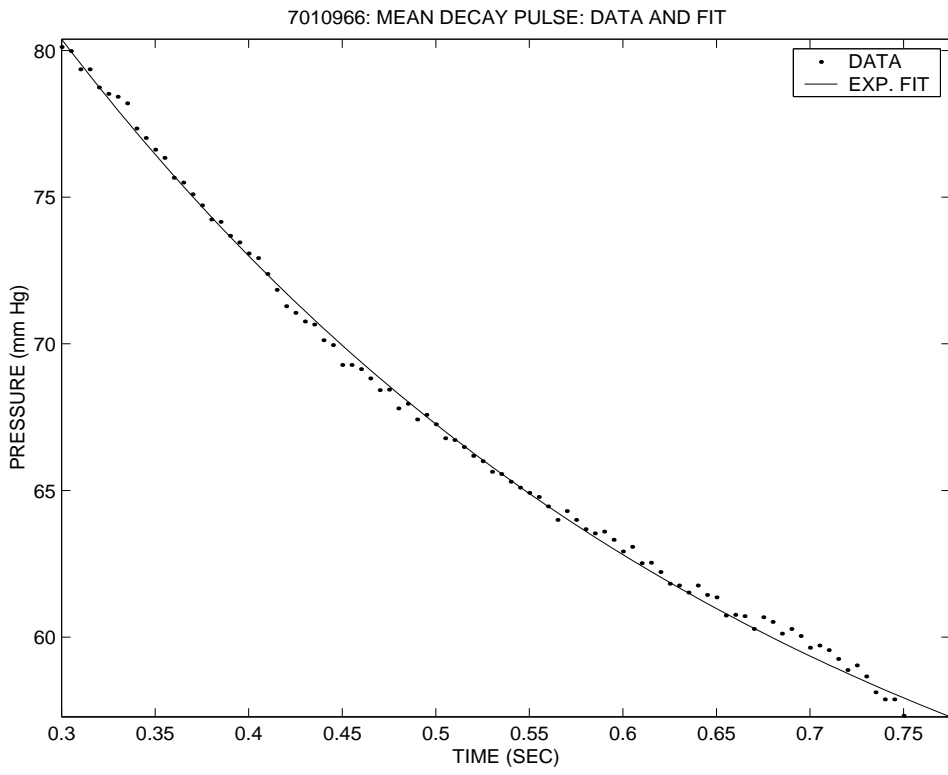


(b)

Figure 23: Data set 7010966: (a) Entire waveform and derivatives. (b) Detected maxima and minima.

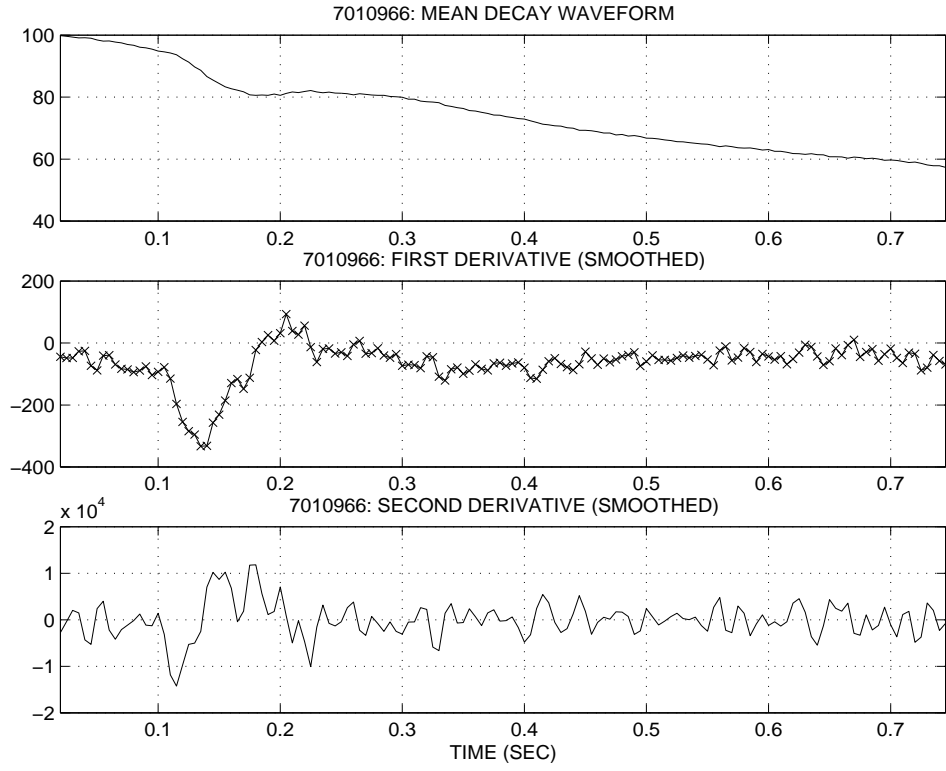


(a)

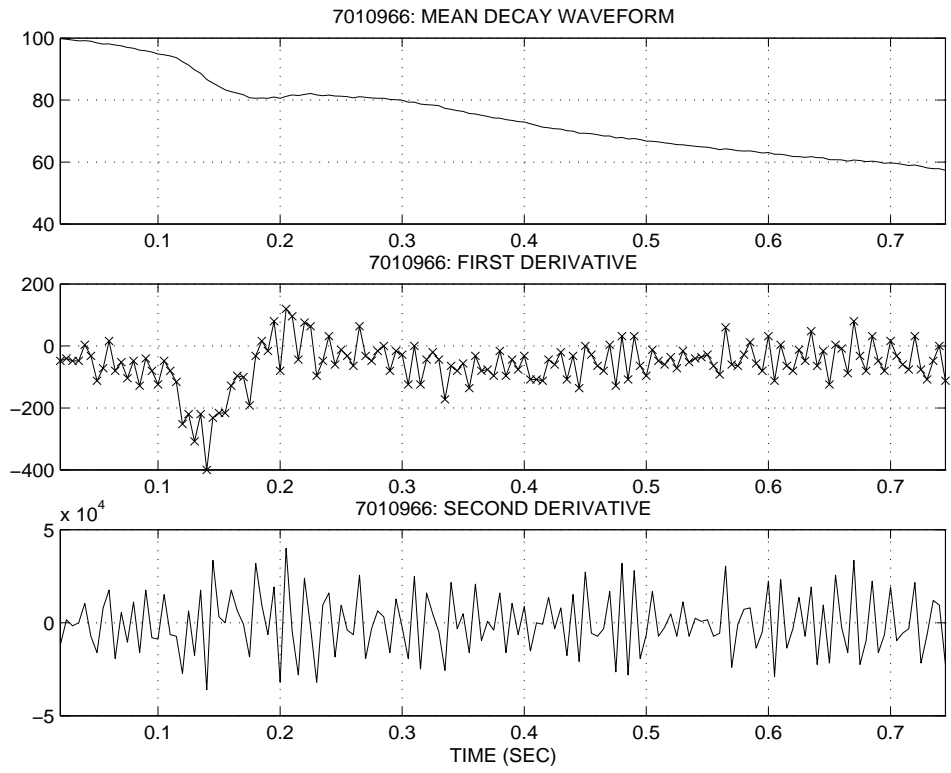


(b)

Figure 24: Data set 7010966: (a) Similar decay waveforms and mean, with detected dichrotic notch indicated by vertical line. (b) Monoexponential fit from notch to diastole.

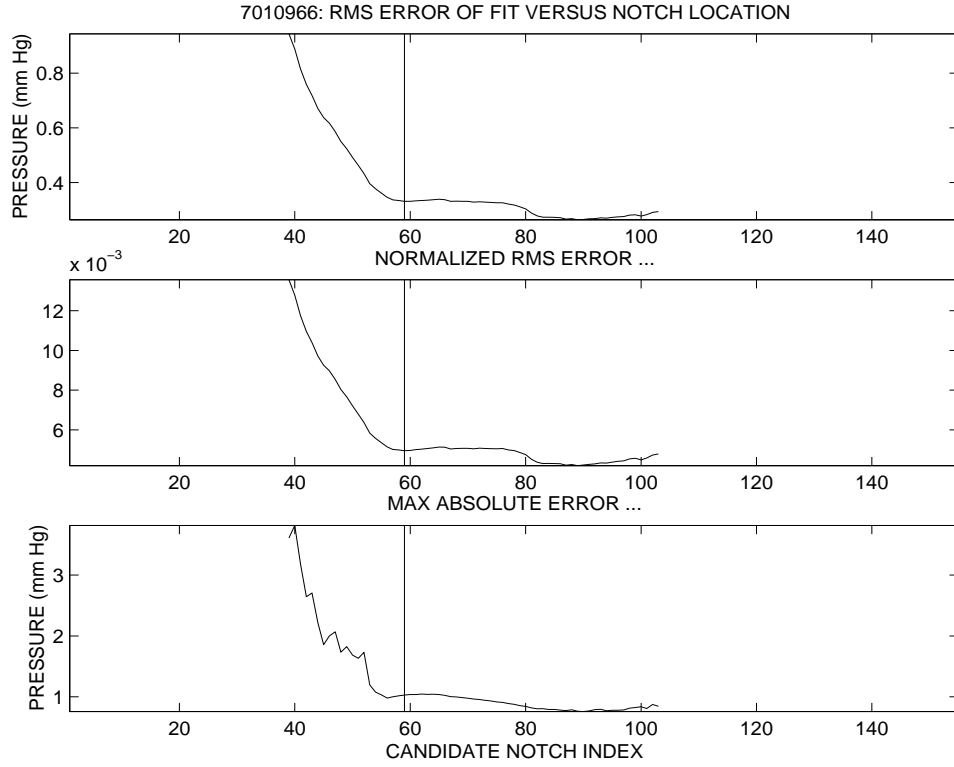


(a)

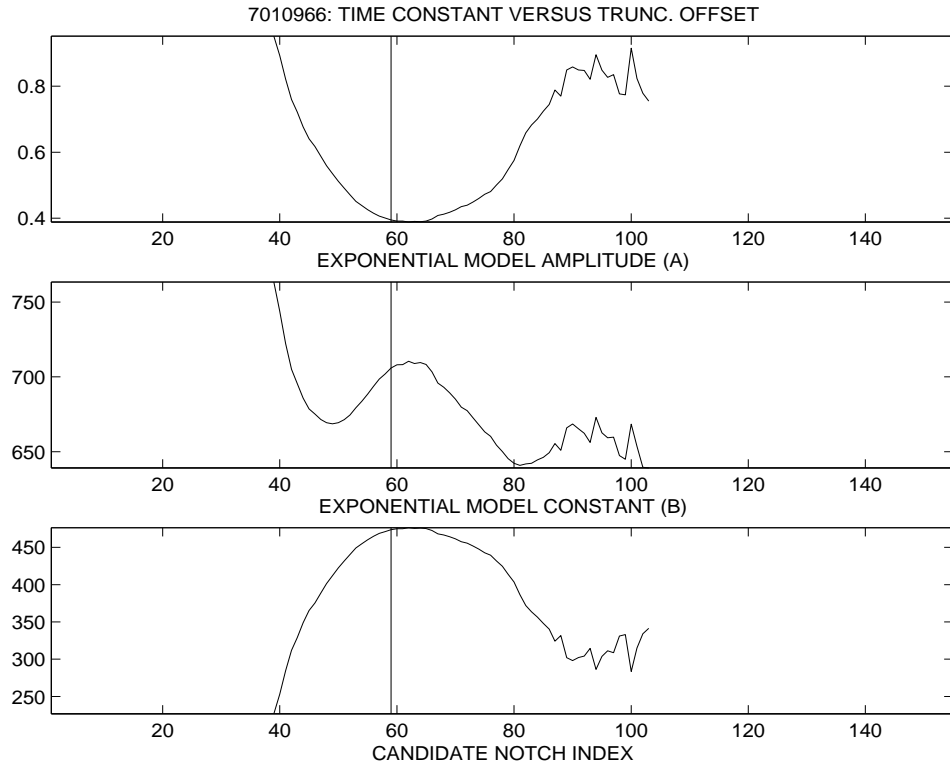


(b)

Figure 25: Data set 7010966: Mean decay waveform and derivatives (a) with and (b) without smoothing.



(a)



(b)

Figure 26: Data set 7010966: (a) Goodness-of-fit measures to exponential model for different choices of dichrotic notch location. (b) Variation in exponential model parameters for different choices of dichrotic notch location.



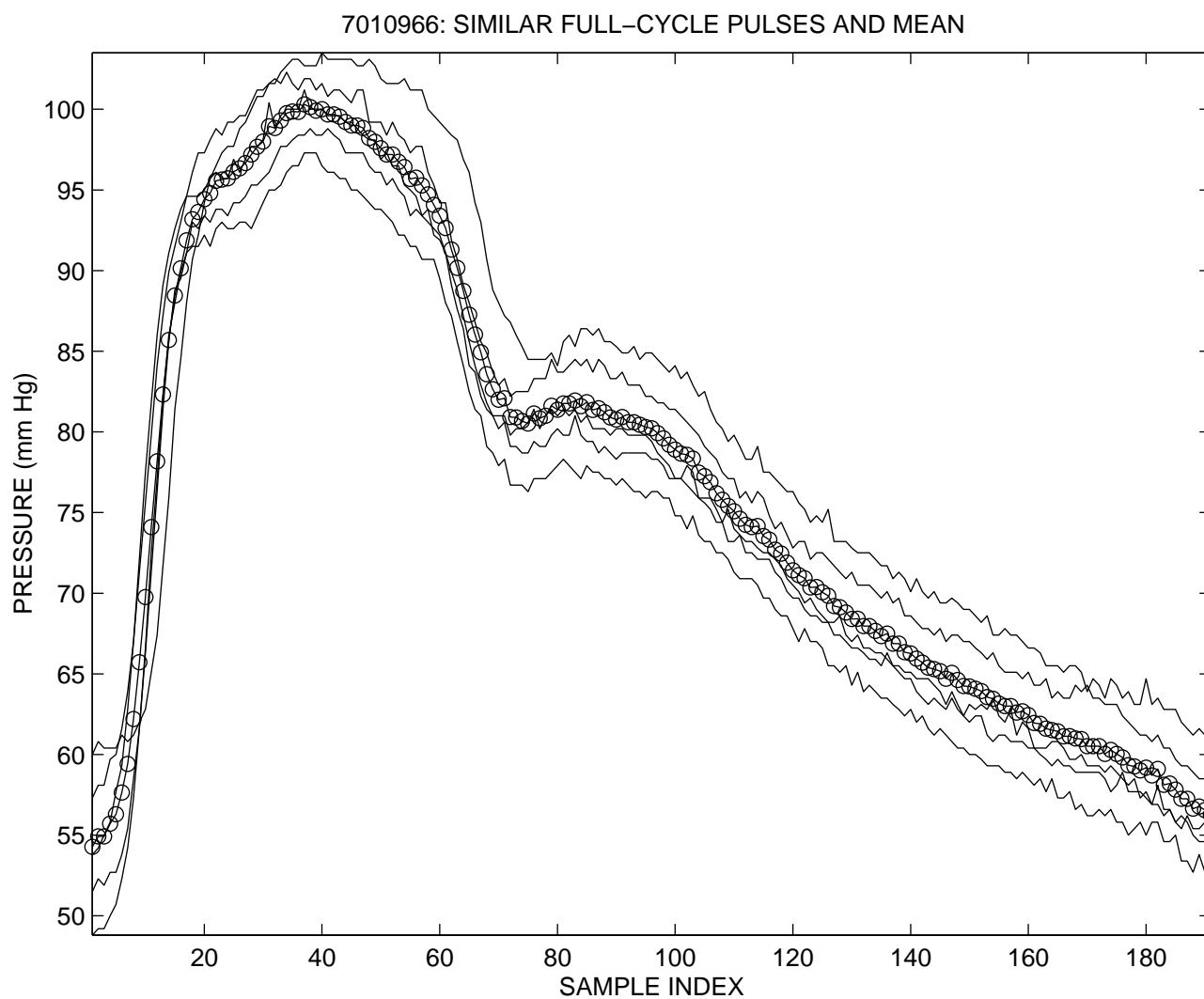


Figure 27: Data set 7010966: Similar full-cycle pulses and mean.

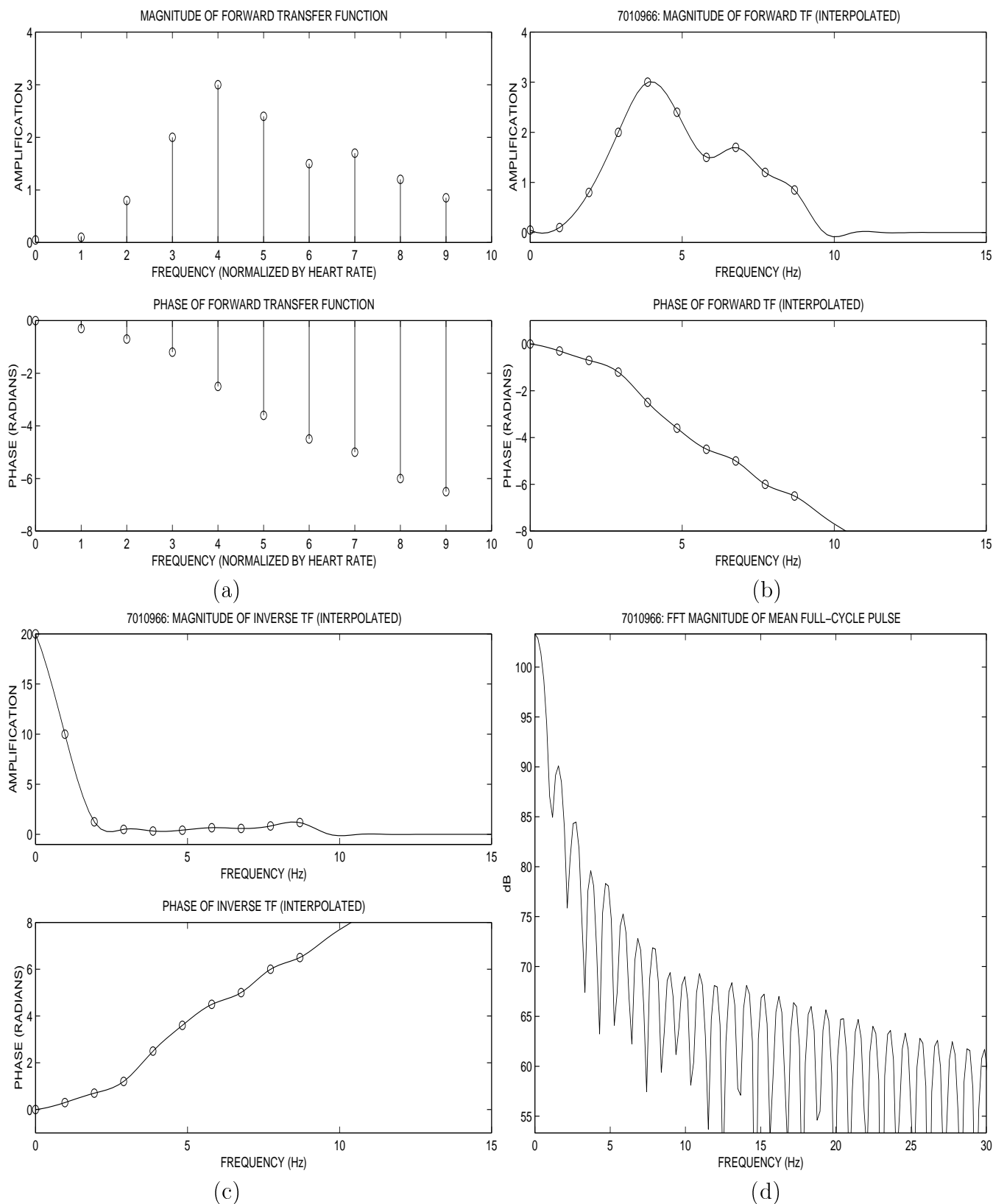
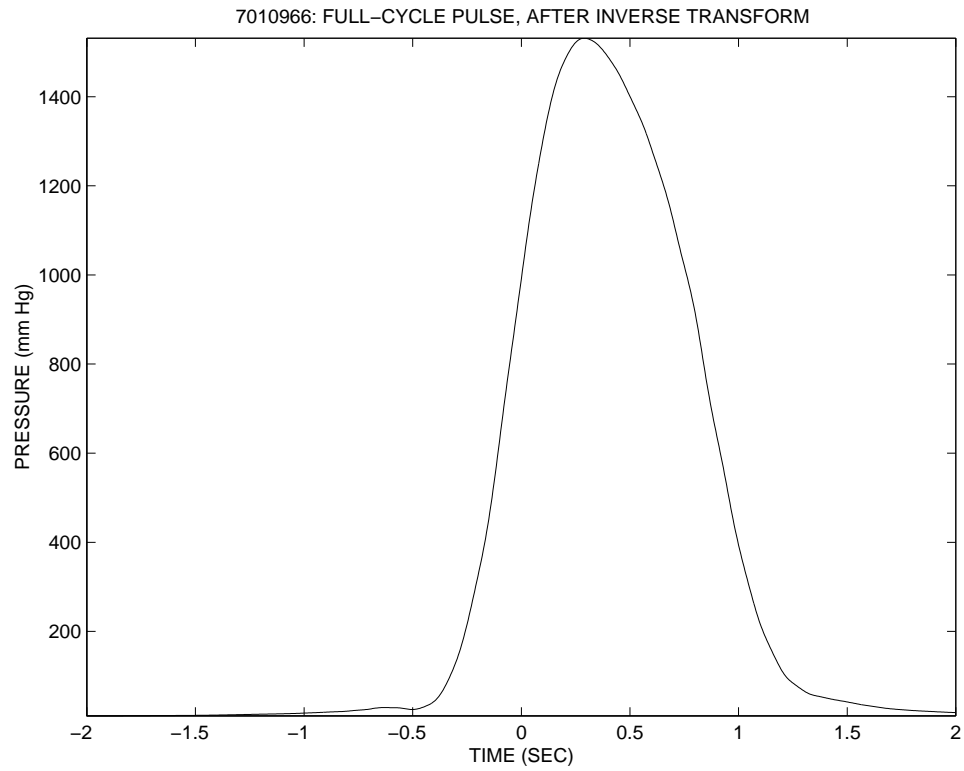
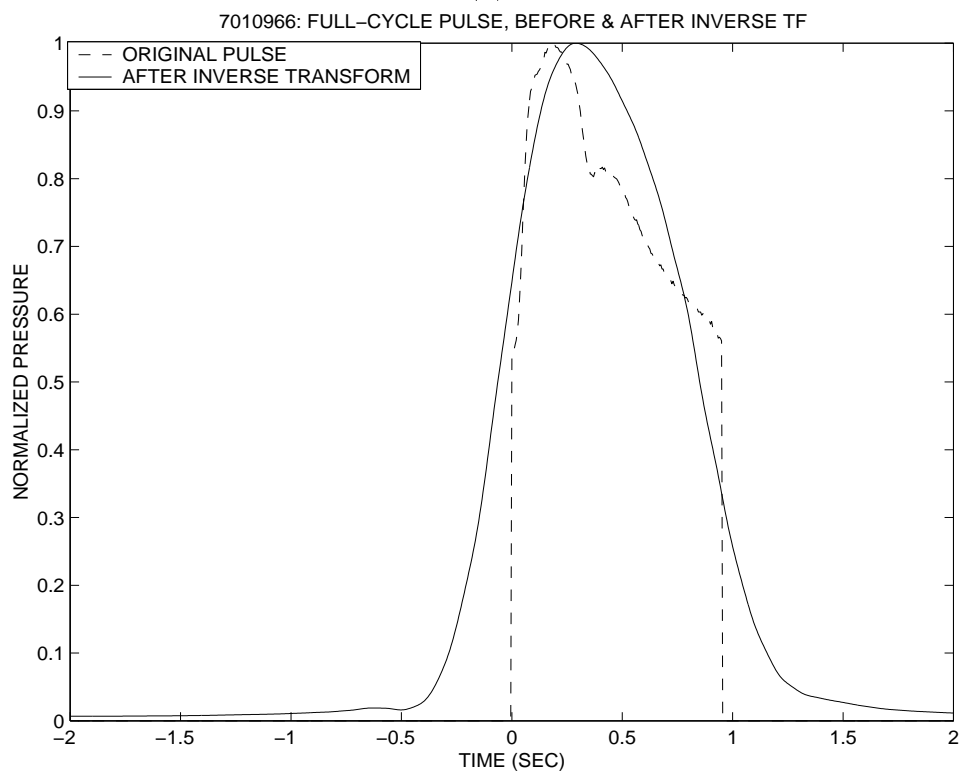


Figure 28: Data set 7010966: (a) Estimate of forward TF, from published graph. (b) Cubic-spline interpolated forward TF. (c) Cubic-spline interpolated inverse TF, with zero gain beyond ninth harmonic. (d) FFT magnitude of mean full-cycle pulse.

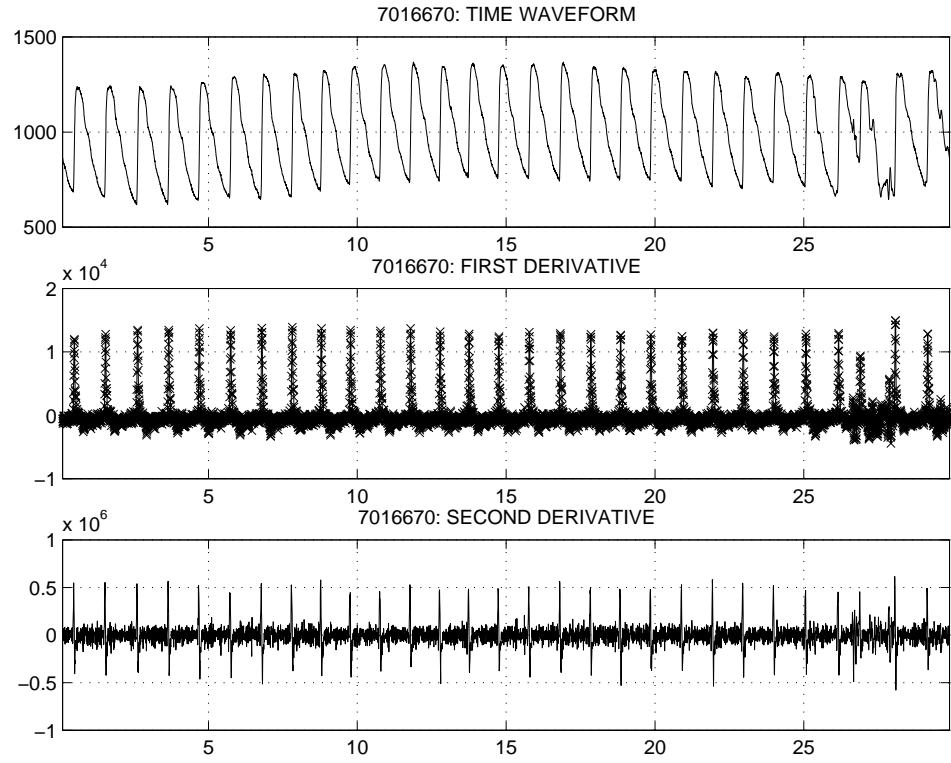


(a)

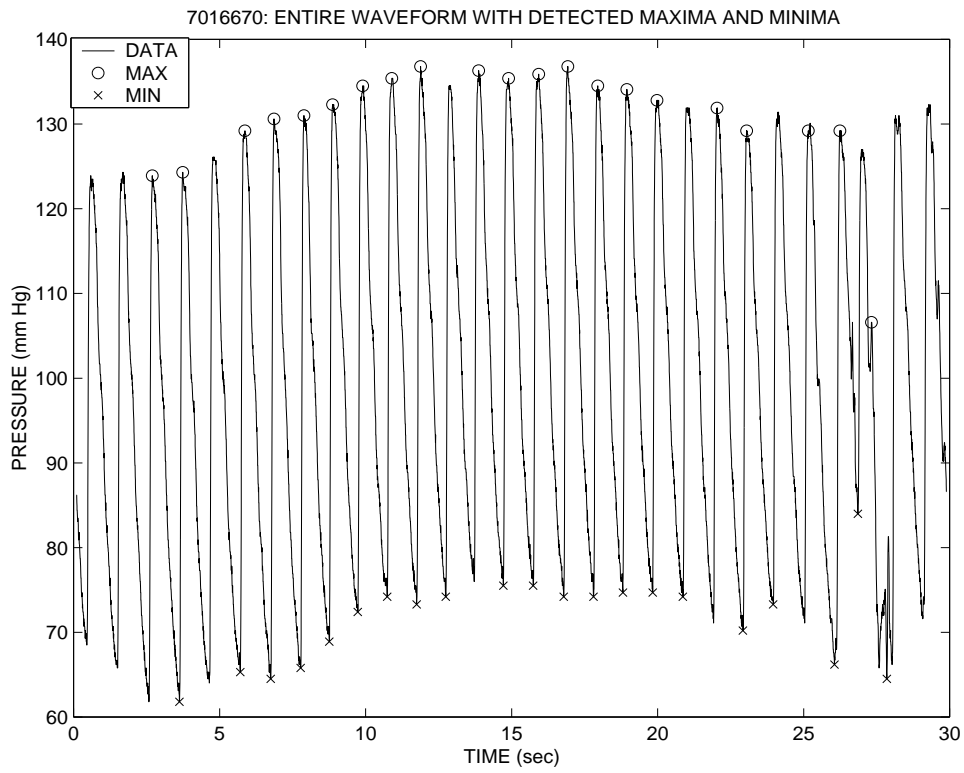


(b)

Figure 29: Data set 7010966: (a) Result of passing mean full-cycle pulse through inverse TF. (b) Full-cycle pulse before and after inverse transform, with peak pressure normalized to 1.

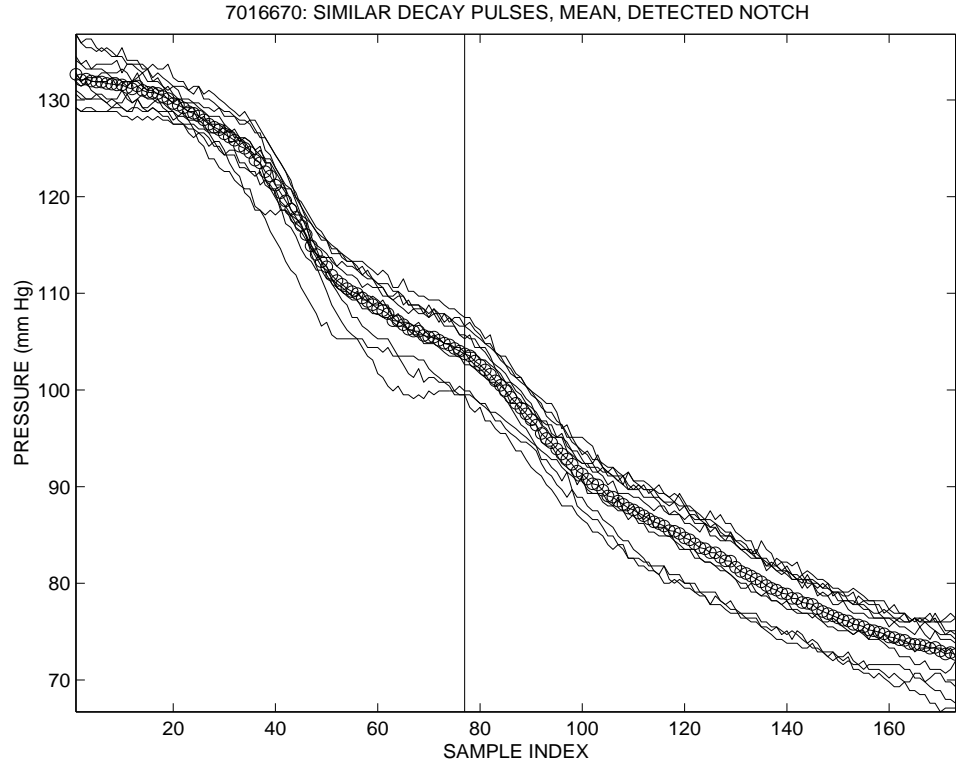


(a)

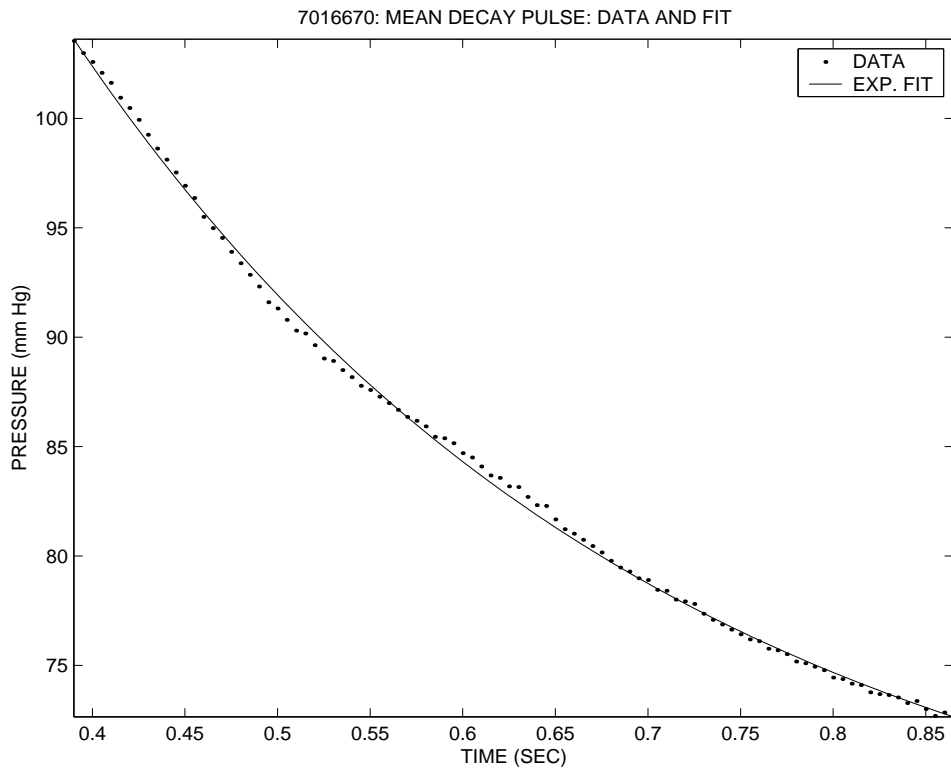


(b)

Figure 30: Data set 7016670: (a) Entire waveform and derivatives. (b) Detected maxima and minima.

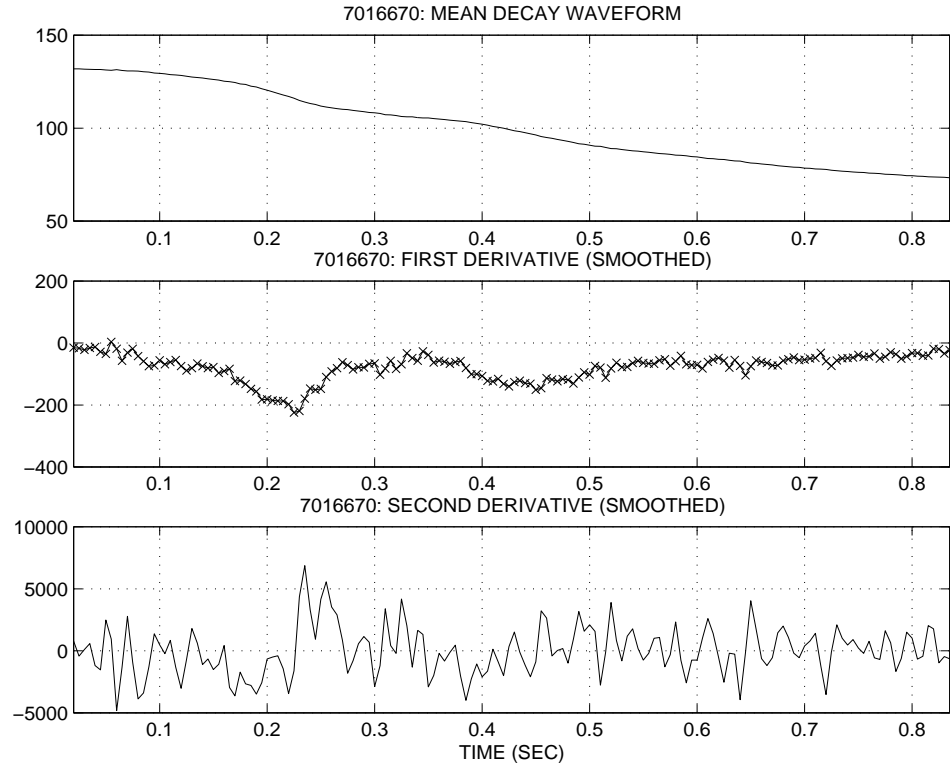


(a)

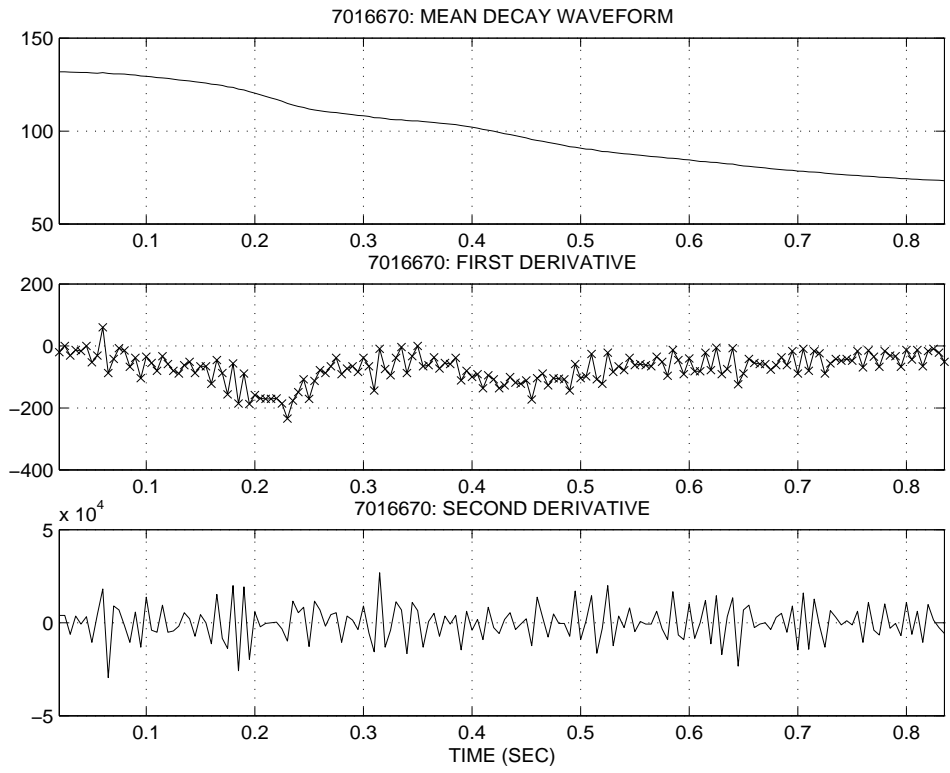


(b)

Figure 31: Data set 7016670: (a) Similar decay waveforms and mean, with detected dichrotic notch indicated by vertical line. (b) Monoexponential fit from notch to diastole.

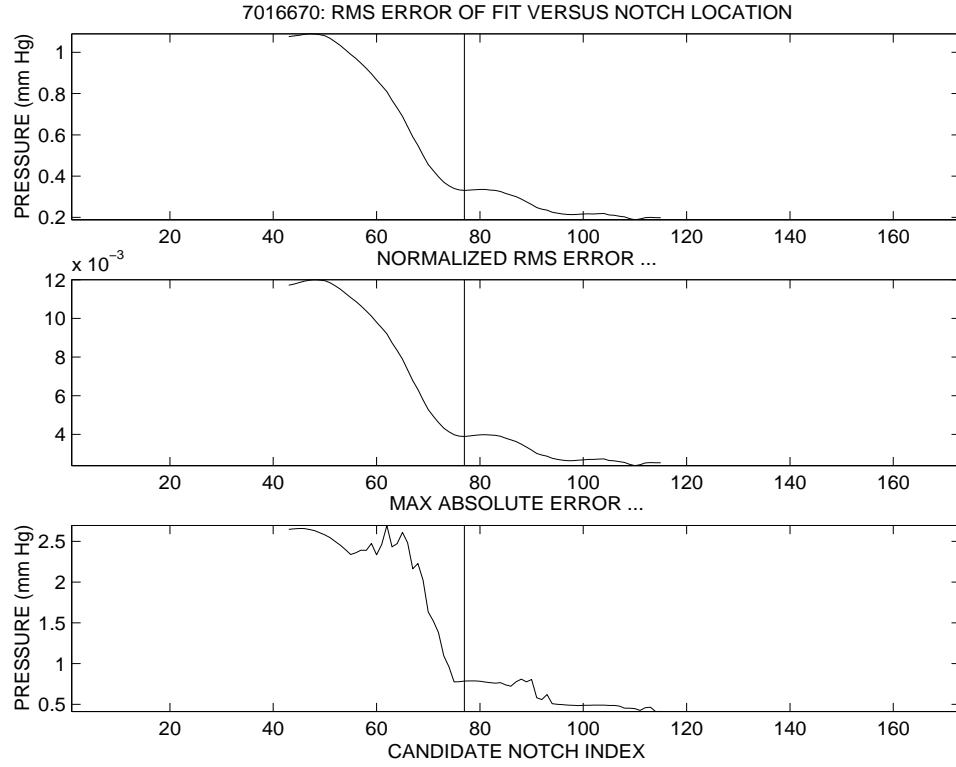


(a)

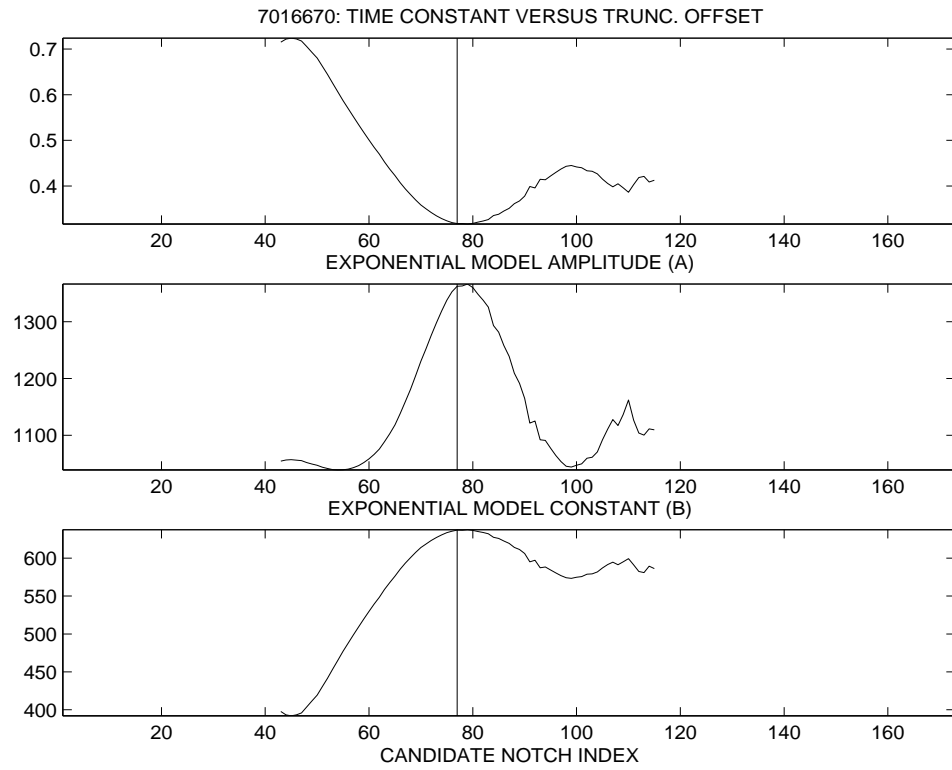


(b)

Figure 32: Data set 7016670: Mean decay waveform and derivatives (a) with and (b) without smoothing.



(a)



(b)

Figure 33: Data set 7016670: (a) Goodness-of-fit measures to exponential model for different choices of dichrotic notch location. (b) Variation in exponential model parameters for different choices of dichrotic notch location.

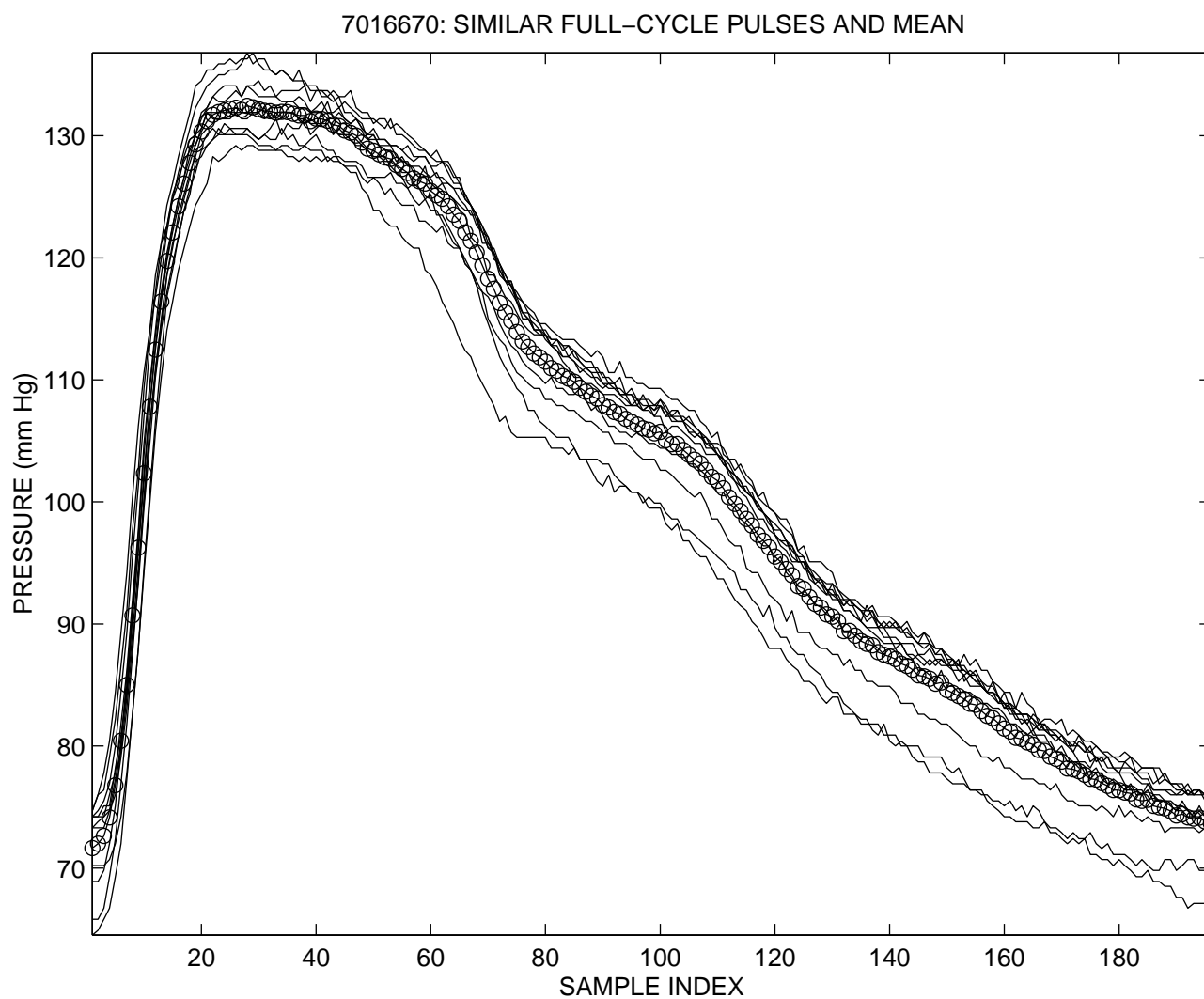


Figure 34: Data set 7016670: Similar full-cycle pulses and mean.



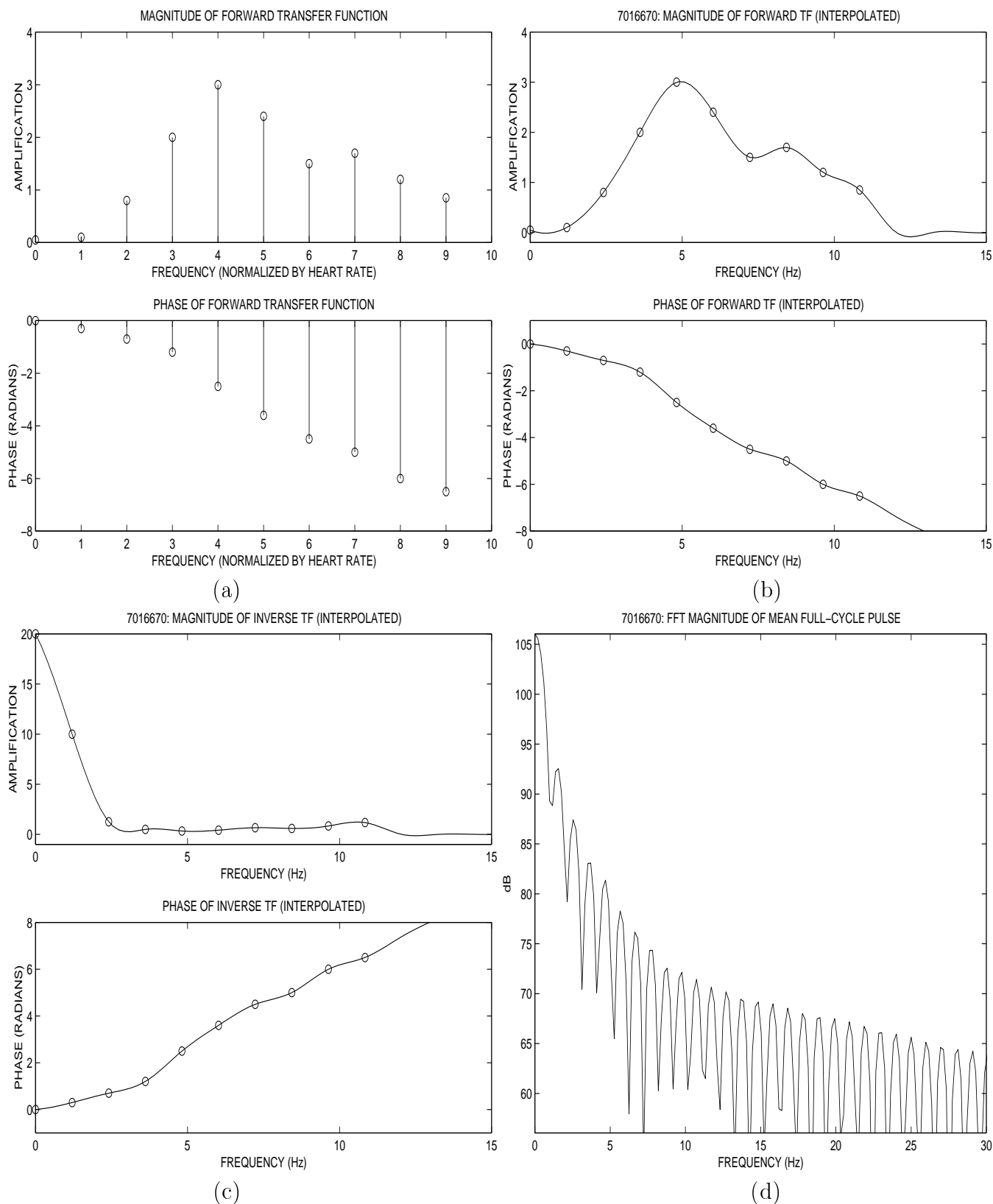
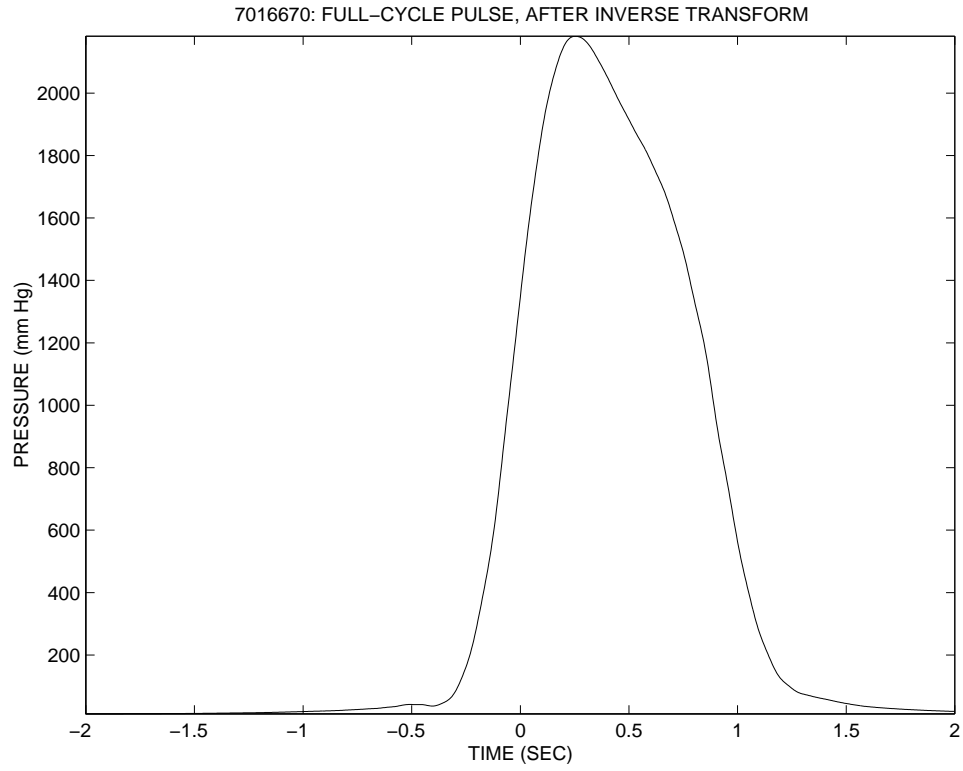
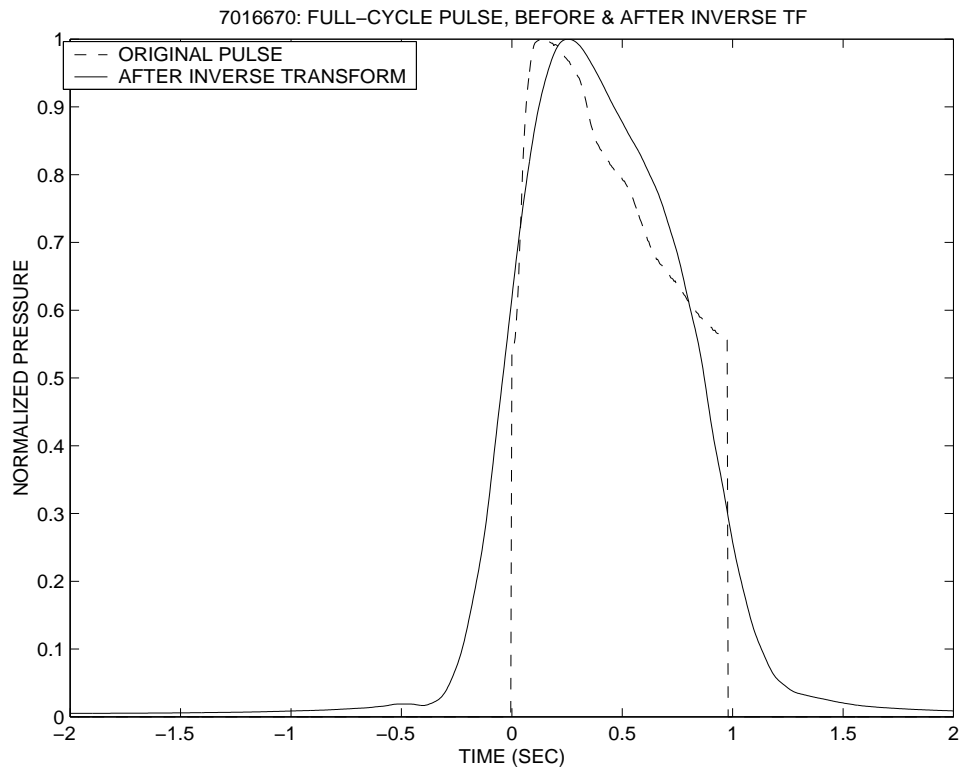


Figure 35: Data set 7016670: (a) Estimate of forward TF, from published graph. (b) Cubic-spline interpolated forward TF. (c) Cubic-spline interpolated inverse TF, with zero gain beyond ninth harmonic. (d) FFT magnitude of mean full-cycle pulse.



(a)



(b)

Figure 36: Data set 7016670: (a) Result of passing mean full-cycle pulse through inverse TF. (b) Full-cycle pulse before and after inverse transform, with peak pressure normalized to 1.